https://doi.org/10.1016/j.tre.2021.102547

Strategic planning of inland river ports under different market structures: Coordinated vs. independent operating regime

Zhi-Chun Li a,*, Mei-Ru Wang a, Xiaowen Fu b

a School of Management, Huazhong University of Science and Technology, Wuhan 430074, China

b Department of Industrial and Systems Engineering, Hong Kong Polytechnic University, Hong Kong, China

Abstract

This paper addresses the strategic planning issue of ports in an inland river corridor with location-dependent waterway depths, which determine the maximum navigable ship sizes deployed in ports. A vertical-structure model is proposed to capture the interrelationships among port operators, carriers, and shippers. The shippers, who are assumed to be continuously distributed along the inland river corridor, choose transshipment ports to minimize their own full transport cost from origin to destination. The carriers aim to maximize their own profit by determining waterway freight rates and ship fleet (in terms of ship size and number of ships). The port operators determine port capacity and port service charge to achieve their own objective, depending on the port market structures adopted, i.e., coordinated vs. independent regime. Under the coordinated regime, the central government aims to maximize total social welfare of the entire inland river system. Under the independent regime, each local government along the inland river corridor maximizes the local social welfare of individual port inside its jurisdiction. The properties of the models with different regimes are analytically explored. Our study develops a comprehensive model that can be used to analyze the investment and regulatory decisions for an inland river shipping corridor composed of multiple heterogeneous ports. The modelling results suggest that local governments have a tendency to overinvest port capacity beyond system optimum. Therefore, in the choice of regulatory regimes, one needs to balance the costs of regulation vs. the avoidance of excessive investments under central government intervention. Findings specific to the Yangtze River inland shipping corridor are also provided.

Keywords: Inland waterway transport; waterway depth; strategic investment; port operating regime.

1. Introduction

1.1. Background and motivation

The Yangtze River of China is the world's largest inland waterway in terms of cargo volume. This "golden waterway" links the country's important inland cities to its major export hubs located in the east coast, playing a crucial role in domestic and international trades. In 2017, the regions along the Yangtze River accounted for 40% and 38% of the national Gross Domestic Product (GDP) and population, respectively (Jiang et al., 2018).[1] Hence, strategic planning of the inland ports along the Yangtze River is of great importance for the regions along the corridor as well as the national economy.

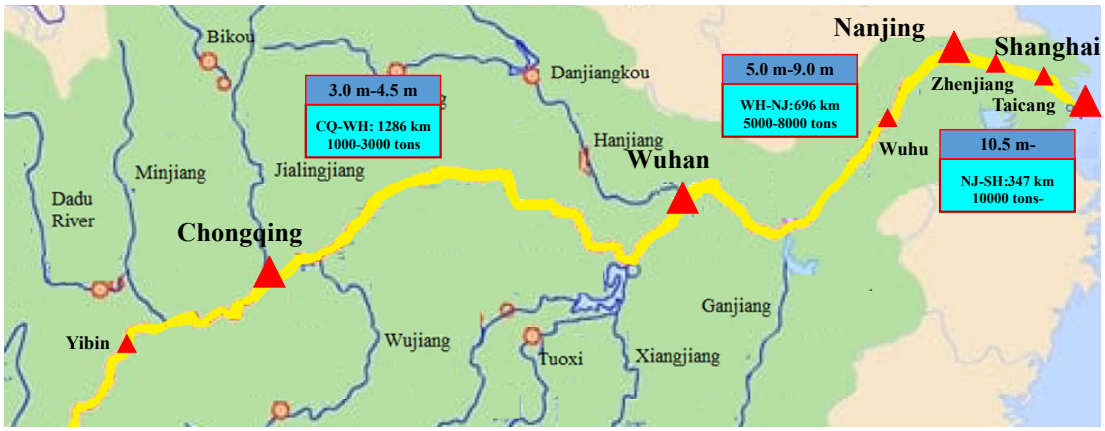

Fig. 1. Major ports and waterway depths along the Yangtze River of China.

There are some major inland river ports along the Yangtze River, such as Nanjing port, Wuhan port, and Chongqing port, as shown in Fig. 1.[2] The waterway depth decreases in order from the downstream port to the upstream port, a pattern commonly observed in other inland shipping markets such as the Mississippi river (Tan et al., 2015). Specifically, the waterway depth between Shanghai port and Nanjing port exceeds 10.5 meters. It declines to 5.0 meters and 3.0 meters on the waterways between Nanjing port and Wuhan port, and between Wuhan port and Chongqing port, respectively. Together with the height restrictions imposed by bridges over the Yangtze River, the different waterway depths lead to heterogeneous shipping capabilities along the river. Seagoing ships with a capacity up to 10,000 tons can navigate

[1] The Yangtze River passes through eight provinces and two municipalities directly under the Central Government, which include Sichuan, Chongqing, Hunan, Hubei, Anhui, Jiangxi, Jiangsu, and Shanghai.

[2] http://www.cjhdj.com.cn/hdfw/ydssjh/202003/t20200326_118342.shtml.

directly to Nanjing port, but cannot sail further to upstream ports, such as Wuhan and Chongqing ports. The maximum navigable ship size at a downstream port is thus often larger than that at an upstream port. Because ships with a larger size usually have a lower variable operating cost but a higher fixed operating cost per unit of cargo, the operating costs of carriers in the Yangtze River are influenced by the waterway depth. This is an important characteristic of inland river shipping and port operation. The present paper accounts for the ship fleet decisions (including ship size and number of ships) of each carrier due to varying waterway depth constraints along the inland river corridor. This is a more realistic and general approach compared to previous inland river shipping studies such as Sauri (2006), Radmilovi et al. (2011), Witte et al. (2012, 2014) and Tan et al. (2015, 2018), which did not consider the effects of waterway depth on fleet decisions.

The rapid growth in cargo volume in the past decade has led to serious congestion at some major inland river ports. For instance, the design capacities of Nanjing port, Wuhan port, and Chongqing port are 200, 95.02 and 96.70 million tons per year, respectively. However, in 2020 the actual throughputs of the three ports already reached 251, 105, and 165 million tons, respectively.[3] This leads to severe port congestion, which is expected to get even worse in the future with continuing growth in cargo volume. Port stakeholders, such as port operators, carriers and shippers, have quite different reactions to port congestion (Meng and Wang, 2011). For port operators, popular approaches to alleviate port congestion include port capacity expansion and port service charge increase (i.e. supply increase vs. demand management). In response to the congestion alleviation strategies of port operators, the carriers may also adjust freight rates and thus the cargo demand. They may also change the deployment of ships at ports to improve transport throughputs and service quality. Shippers also play active roles in determining market equilibrium by choosing transshipment ports to minimize their own full transport cost from origin to destination. In summary, all these stakeholders' interrelated decisions have significant impacts on the market outcome, and should be explicitly considered when modelling long-term development plans.

Ownership and institutional factors are important factors in port operation. The ports along the Yangtze River are currently managed by local governments, who consider ports as a driver of the local economy. They may adjust service charge and capacity to ensure that their own ports are well-positioned in the competition. In addition, the central government also

[3] https://www.mot.gov.cn/tongjishuju.

establishes a special administrative institution named "Changjiang River Administration of Navigational Affairs (CRANA)", which coordinates the operations of all ports along the Yangtze River in an integrated manner. The CRANA's responsibilities include making strategic development and investment plans of the river waterway system, overseeing water safety, operations and management of information and rescue systems, and enforcement of waterway law (Jiang et al., 2018). Under the mandate of the central government, CRANA aims to maximize the total social welfare of the inland river corridor system by coordinating port service charges and capacities of all ports in the river system. Intuitively, such a "social planner" approach would lead to socially optimal outcome at the national level. On the other hand, it is well-known that competition often leads to significant gains through efficient services in the long term (Amsden and Singh, 1994; Blaug, 2001), whereas direct government intervention often comes with regulatory cost. Therefore, it is important to evaluate and compare the market outcomes under different management and market structures, such as coordinated (centralized) management vis-a-vis independent (decentralized) local government management. This study aims to achieve this objective by analytically model and compare these alternative regimes.

1.2. Literature review

In the literature, a number of studies have investigated the strategic planning of ports. Table 1 summarizes some of the principal contributions to the modeling of ports in a continuum corridor, notably the type of ports, demand distribution, number of ports, effects of waterway depth, stakeholders, port operating regime(s), and decision variable(s). Table 1 shows that the previous studies have mainly focused on seaports, with limited attention paid to inland river ports for which the waterway depth and thus the maximum navigable ship size change with port location along the river. That is, there are exogenously imposed constraints which contribute to port asymmetry. Two exceptions are Tan et al. (2015, 2018), which nevertheless did not consider the effects of location-dependent waterway depth on the decisions of stakeholders in the corridor system. Moreover, only one or two ports were considered in previous studies. Such a simplification could potentially limit the model applicability to markets with multiple ports, such as the inland river shipping system along the Yangtze River.

As summarized in Table 1, previous studies usually assumed a uniform cargo demand distribution along the river corridor. Such a strong assumption is useful for deriving

Table 1 Principal contributions to modeling of ports in a continuum corridor.

Reference	Type of ports	Demand distribution	Number of ports	Considering effects of waterway depth	Stakeholders concerned	Port operating regime(s) concerned	Decision variable(s)
Basso and Zhang (2007)	Seaports	Uniform	Two	No	Port operator, carrier and shipper	Coordinated and independent private operations, central government	Port service charge and capacity, waterway freight rate
Kaselimi et al. (2011)	Seaports	Uniform	Two	No	Port operator and shipper	Independent local governments	Port service charge and capacity
Homsombat et al. (2013)	Seaports	Uniform	Two	No	Port operator, carrier and shipper	Independent private operations	Port service charge and waterway freight rate
Zerny et al. (2014)	Seaports	Uniform	Two	No	Port operator and shipper`	Independent private and local governments	Port service charge
Tan et al. (2015)	Inland river port	Uniform	One	No	Port operator and shipper	One private operator	Port service charge and capacity
Álvarez-SanJaime et al. (2015)	Seaports	Uniform	Two	No	Port operator and shipper	Coordinated and independent private operations, central government	Port service charge
Wan et al. (2016)	Seaports	Uniform	Two	No	Port operator and shipper	Central and independent local governments, independent private operations	Port service charge and road capacity
Tan et al. (2018)	Inland river port	Exponential	One	No	Port operator and shipper	One private operator	Port service charge
Xing et al. (2018)	Seaports	Uniform	Three	No	Port operator and shipper	Independent local governments	Port service charge
Trujillo et al. (2018)	Seaports	Uniform	Two	No	Port operator and shipper	Coordinated and independent private operations	Port service charge and capacity
This paper	Inland river ports	Exponential, Uniform	Any N	Yes	Port operator, carrier and shipper	Coordinated and independent governments	Port service charge and capacity, waterway freight rate and ship fleet

closed-form solutions. However, the heterogeneity of cargo demand by port location cannot be considered with this simplification. In reality, the cargo demand distribution along a river corridor may depend very much on the geographical locations of inland ports, population size and socio-economic development of inland port cities.

In addition, the existing studies usually considered only two stakeholders (i.e., port operator and shipper), with the role of carrier largely ignored. This may introduce distortions in modelling results, because carriers' choices of ship fleet and waterway freight rate can significantly affect the decisions of port operator and shipper. There is indeed a need to explicitly consider the interactions among port operator, carrier and shipper, such that the models developed can capture the intrinsic characteristics of the river corridor system.

1.3. Problem statement and contributions

In view of the aforementioned industry needs and research gaps, this paper investigates the strategic planning problem of the ports along an inland river corridor. We consider a linear inland river corridor connecting a destination port with some major upstream ports, as shown in Fig. 2. For ease of presentation, these ports are numbered as 0, 1,…, *i*,…, *N*, where *i* denotes a port, and "*i* = 0" denotes the destination port (e.g., Shanghai port which handles many transshipments). There are two alternative routes to the destination port for the cargo demand originating at any location *x* between adjacent ports *i* and *i*+1, i.e., Routes I and II. For Route I, the cargos are first transported to downstream port *i* via road transport and then to the destination port via waterway transport. For Route II, the cargos are first transported to upstream port *i*+1 via road transport and then to the destination port via waterway transport. The choice of shipping route is an important decision for each shipper in minimizing the full transport cost from origin to the destination.

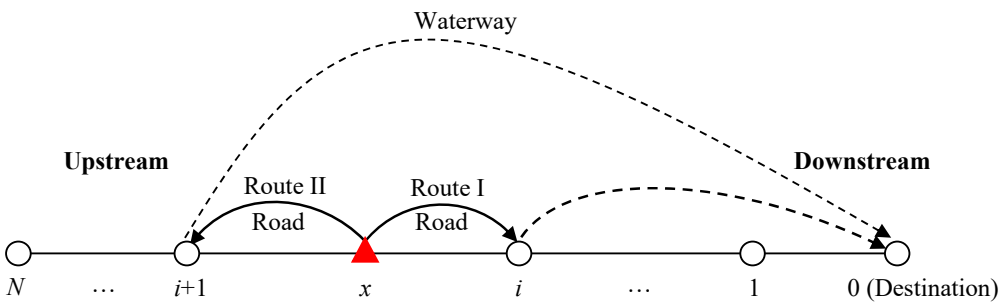

Fig. 2. Port configuration and route choice in an inland river corridor.

There exist three types of stakeholders in the inland river system: shippers, carriers and port operators. The vertical-structure relationships among them are shown in Fig. 3, and are explained as follows. The shippers are modelled to be continuously distributed along the inland river. They choose the intermodal chain or route (hinterland transport plus transshipment port) to minimize their own full transport cost. The carriers compete for cargo demand, with an objective to maximize their individual profit by determining the waterway freight rate and the ship fleet (in terms of ship size and number of ships). The port operators provide port services to carriers, and set port service charge and port capacity to achieve their own objective, depending on the port operating regimes adopted. In this paper, we consider two kinds of port operating regimes, namely the coordinated (or centralized) regime vis-à-vis the independent (or decentralized) regime. Under the coordinated regime, all ports along the inland river are controlled by the central government, with an objective of maximizing total social welfare of the entire inland river system. Under the independent regime, each port along the inland river is operated by the corresponding local government that aims to maximize the local social welfare within its jurisdiction. The different stakeholders' objectives and the vertical structure are presented in Figure 3.

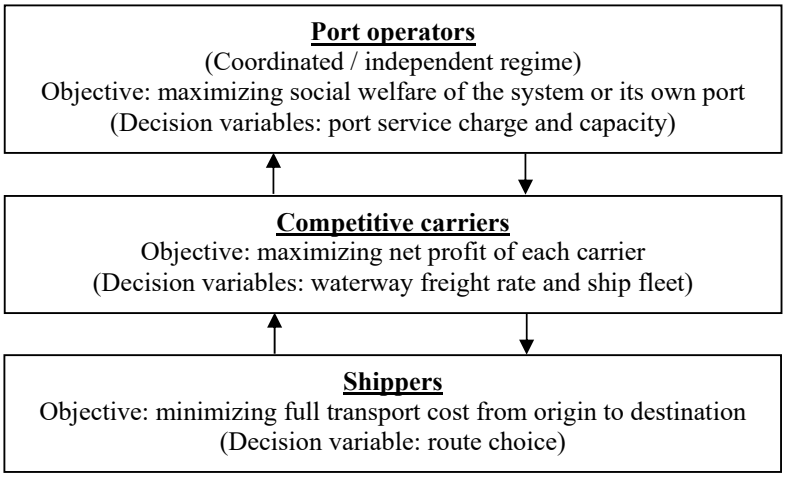

Fig. 3. Vertical-structure relationships among shippers, carriers and port operators.

The main modelling contributions of this paper are twofold. First, in terms of methodology a vertical-structure model with a general specification of cargo demand distribution and the port congestion is proposed, which models the determination of port service charge and capacity, waterway freight rate, and ship fleet (ship size and number of ships) for multiple ports of an

inland river system. The interactions among different stakeholders, including port operators, carriers and shippers, are explicitly considered. The ship size is confined by the location-dependent waterway depth. Overall, our model is more comprehensive and considers a more general and realistic inland shipping market. Such a framework allows us to investigate complex issues for inland shipping. For example, different port operating regimes, including coordinated (centralized) and independent (decentralized) regimes, are investigated and compared. The properties of the models with different operating regimes are analytically explored, notably for the case of uniform cargo demand distribution and no port congestion. The interrelationships among some key parameters or factors, such as waterway depth, port service charge, port capacity investment, waterway freight rate, and port operating regimes, are also explored, together with their implications in practice. Second, this study provides some important managerial and regulatory insights. For example, we have shown that the optimal capacity expansion of each port under the independent regime is always larger than that under the coordinated regime. This is because each independent government needs more port capacities to compete for hinterland cargo market with rivals. This conclusion may have very important implications for inland port investment and choice of regulation schemes. Regulation always comes with costs (e.g. regulation costs associated with tax collection, administration etc.). When the cargo demand along the inland river is expected to grow substantially in coming years, limited over-investments may not be a major problem. In such a case, encouraging competition is a preferred solution than central management / coordination. However, if market growth is expected to be limited in the years to come, regulation cost is a less important issue compared to wastes caused by excessive investments. In such a case, centralized regulation/coordination may be a preferred choice. Because such results are obtained under general modelling assumptions, they should hold for inland river shipping in general.

The rest of the paper is organized as follows. Section 2 describes some basic components of the proposed models, including model assumptions, full transport cost, and cargo demand density. The vertical-structure models with general specifications of cargo demand distribution, number of ports and port congestion under coordinated and independent regimes are presented in Section 3. Section 4 discusses the solution properties of the models for a special case with uniform cargo demand distribution and no port congestion. In Section 5, numerical examples are used to illustrate the properties and applications of the proposed models. Section 6 draws conclusions and offers recommendations for further studies.

2. Basic components of the models

2.1. Assumptions

To facilitate the presentation of the essential concepts without the loss of generality, the following basic assumptions are made in this paper.

A1 The inland river is considered as a linear continuum transport corridor (Li et al., 2012; Tan et al., 2015). The cargos (or equivalently, shippers) are assumed to be continuously distributed along the continuum corridor and they can be only transshipped at most once.

A2 For simplicity, each port is assumed to have only one carrier or one carrier alliance (e.g., Meng et al., 2012; Wang et al., 2014a; Sheng et al., 2017), who decides on the ship type and the number of ships adopted and the waterway freight rate to maximize its own profit. All shippers in a port are assumed to have the same preferences, i.e., the same transport cost function and the same value of time (Tan et al., 2015; Wan et al., 2016).

A3 The transport cost per unit of cargo consists of the transport time cost (port congestion delay cost, in-transit time cost for road / waterway transport) and the monetary cost for road / waterway transport. The marginal cost of road transport is assumed to be exogenously given, as assumed in Tan et al. (2015) and Dai et al. (2018).

A4 The port capacity is influenced by the equipment of handling cargos, such as cranes for loading and unloading cargos, scrapers for moving cargos, and warehouse of storing cargos (Tan et al., 2015). Port congestion delay depends on the total cargo volume and the capacity of that port, and is assumed to be a linear function of the ratio of cargo volume to port capacity (Wan et al., 2015; Basso and Zhang, 2007; Sheng et al., 2017; Wang and Meng, 2019).

2.2. Full transport cost of shippers

As shown in Fig. 2, there are two alternative routes (i.e., transshipping via downstream or upstream port) for each shipper at any location x between adjacent ports i and i+1 to transport his/her cargos to the destination port. Let $c_i(x)$ and $c_{i+1}(x)$ be the full transport cost per unit of cargo (e.g. per TEU container handled) from location x to the destination through transshipping the cargos at downstream port i and upstream port i+1, respectively. According

to **A3**, the full transport cost, $c_i(x)$, consists of the time cost (port congestion delay cost, in-transit time cost for road / waterway transport) and the monetary cost for road / waterway transport, expressed as

$$c_i(x) = c_i^R(x) + g_i + p_i D_i + \alpha_3 t_i D_i, \tag{1}$$

where the superscript "R" represents the road transport. $c_i^R(x)$ is the road transport cost from location x to port i. g_i is the congestion delay cost of port i due to imbalance between demand and supply. p_i is the waterway freight rate per unit cargo (e.g. per container or one ton of cargo) per unit of distance charged by carrier i, and D_i is the sailing distance between port i and the destination port. $p_i D_i$ is thus the total monetary expenditures paid to carrier i. α_3 is the value of waterway transit time perceived by shippers. t_i is the voyage time per unit of distance for the ships in port i. The term $\alpha_3 t_i D_i$ is thus the voyage time cost per unit of cargo from port i to the destination port. For the convenience of readers, all variables and parameters used throughout this paper are defined in Appendix A.

In Eq. (1), the road transport cost, $c_i^R(x)$, from location x to downstream port i is composed of a distance-based road freight rate and a corresponding transit time cost, defined as

$$c_i^R(x) = c^R(x - D_i) + \alpha_1 t_0^R(x - D_i), \tag{2}$$

where $x - D_i$ is the road transport distance. c^R is the road freight rate of one container (or one ton of cargo) per unit of distance, which can be obtained from industrial statistical data. α_1 is the value of road transport time. t_0^R is the road transport time per unit of distance.

The voyage time cost, $\alpha_3 t_i D_i$, from port i to the destination port depends on the ship size because different types of ships (or ship sizes) usually have different voyage speeds. Some empirical studies have shown that average voyage time t_i per unit of cargo and ship size V_i have a relationship of power or linear function (see Xing et al., 2016; Brown and Aldridge, 2019). Moreover, it is widely recognized that scale economy effects exist between voyage time t_i and ship size V_i. To reflect the scale economy effects, the average voyage time t_i per unit of cargo is defined as

$$t_i = \lambda_0 V_i^{-\lambda_1}, \text{ with } t_i^{\min} \le t_i \le t_i^{\max}, \ \lambda_0, \lambda_1 > 0, \tag{3}$$

where λ_0 is a positive parameter for describing the relationship between the ship size of a port and its voyage time. λ_1 measures the scale economies of the voyage time per unit of cargo about the ship size. $t_i^{\min}$ and $t_i^{\max}$ are, respectively, the lower bound and upper bound of voyage time t_i, which are used to guarantee safe navigation between ships. For example, $t_i^{\min}$ and $t_i^{\max}$ in the Yangtze River are, respectively, set as 0.04 h/km and 0.13 h/km (Fan et al., 2015).

Ship size V_i to be deployed at port *i* is related to the waterway depth of that port. It cannot exceed the maximum navigable ship size, $V_i^{\max}$, of port *i*, which is confined by its waterway depth H_i. Without loss of generality, the relationship between $V_i^{\max}$ and H_i is specified as

$$V_i^{\max} = \eta H_i, \tag{4}$$

where η is a positive parameter for describing the relationship between maximum navigable ship size of a port and its waterway depth.

The congestion delay g_i of port *i* generally decreases with its capacity or throughput, but increases with its total cargo volume. According to **A4,** it can be expressed as

$$g_i = \frac{\alpha_2 Q_i}{K_i}, \tag{5}$$

where α_2 is the value of port congestion time perceived by shippers. K_i is the design capacity of port *i*. Q_i is annual actual total cargo volume of port *i*, defined later.

In light of the above, $c_i(x)$ in Eq. (1) can be rewritten as

$$c_i(x) = (c^R + \alpha_1 t_0^R)(x - D_i) + \frac{\alpha_2 Q_i}{K_i} + (p_i + \alpha_3 \lambda_0 V_i^{-\lambda_1}) D_i. \tag{6}$$

Similarly, the full transport cost, $c_{i+1}(x)$, for transshipping the cargos via upstream port *i*+1 can be expressed as

$$c_{i+1}(x) = (c^R + \alpha_1 t_0^R)(D_{i+1} - x) + \frac{\alpha_2 Q_{i+1}}{K_{i+1}} + (p_{i+1} + \alpha_3 \lambda_0 V_{i+1}^{-\lambda_1}) D_{i+1}. \tag{7}$$

2.3. Cargo demand density

Cargo demand is generally sensitive to the waterway freight rate and the port service level. In literature, a negative exponential elastic demand density function is usually adopted to model the cargo demand elasticity (see e.g., Zlatoper and Austrian, 1989; Wang et al., 2014b; Tan et al., 2018), which is also used in this paper. Let $q_i(x)$ be the annual density of the actual cargo demand originating at location *x* and transshipping at port *i*, expressed as

$$q_i(x) = q^0(x)\exp\left(-\xi c_i(x)\right), \quad x \in [S_{i-1}, S_i], \tag{8}$$

where $q^0(x)$ is the annual potential cargo demand at location *x*. As $q^0(x)$ is a constant, e.g., $q^0(x) = q_0$, the potential cargo demand along the inland river corridor follows a uniform distribution. ξ is the demand elasticity for measuring the sensitivity of cargo demand with respect to the full transport cost per unit of cargo. The larger the value of ξ, the smaller the actual cargo demand, and vice versa. In particular, as ξ equals 0, cargo is insensitive to the full transport cost per unit of cargo, meaning that the actual cargo demand equals the potential cargo demand. $[S_{i-1}, S_i]$ is the catchment (or hinterland) area of port *i* on the inland river, which will be defined later.

3. Model formulation

In this section, we present a general model with general specifications of cargo demand distribution, number of ports and port congestion. As previously stated, the relationships among stakeholders in the inland river system can be represented as a vertical structure, in which the port operators determine the port service charge and port capacity to maximize the total (or local) social welfare under the coordinated (or independent) regime; the carriers set their own waterway freight rate and ship fleet responding to the waterway depth, port operators' service charge, and shippers' cargo demand distribution; and the shippers choose the transshipment port or route to minimize their own full transport cost. In the following, we formulate the interrelated decisions of these stakeholders one by one, beginning with the shippers' decisions.

3.1. Full cost minimization problem for shippers

Shippers at any location $x \in [D_i, D_{i+1}]$ of the corridor may choose to transship at downstream

port *i* or upstream port *i*+1, depending on which port leads to the lowest full transport cost. At the equilibrium state, there exists a watershed or indifference location between ports *i* and *i*+1 such that the full transport costs via the downstream and upstream ports are equal. In order to ensure that each port has the cargo demand, the watershed location should be in between ports *i* and *i*+1. Let S_i represent the watershed location between ports *i* and *i*+1, measured by the distance of the watershed location from the destination port location 0. S_i can be determined by letting $c_i(S_i) = c_{i+1}(S_i)$ for any $i = 0,1,\cdots,N-1$ and S_N can be calculated by letting $c_N(S_N) = b$, where *b* denotes the maximum acceptable full transport cost (or willingness to pay) for shippers.

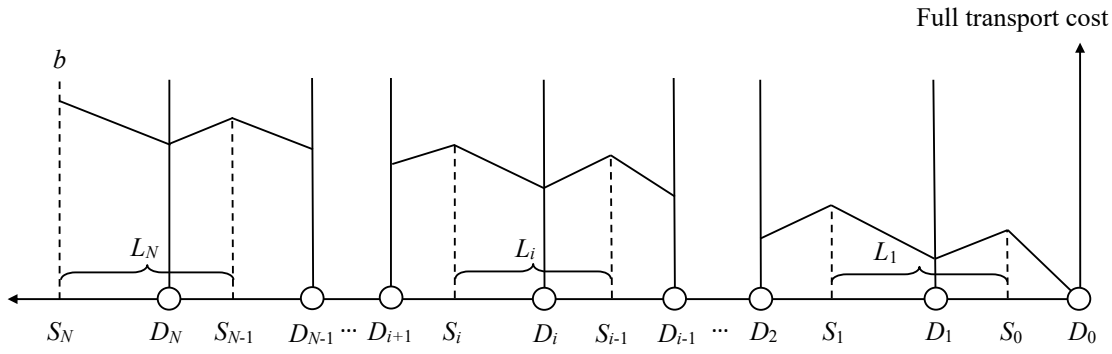

Fig. 4. Catchment areas of ports along the inland river corridor.

For illustration purpose, Fig. 4 shows the catchment (or hinterland) area $[S_{i-1}, S_i]$ of any port *i* along the inland river. Beyond S_N (i.e., the upstream watershed location of port *N*), there are no shippers who would like to use water transport due to excessively high full transport cost (i.e., higher than willingness to pay). Beyond S_0 (i.e., between S_0 and D_0), shippers choose a pure road system to transport directly their cargos to the destination port.

Based on Eqs. (6) and (7), and the indifference conditions of the watershed locations ($c_i(S_i) = c_{i+1}(S_i), i = 0,1,2,\cdots,N-1$ and $c_N(S_N) = b$), one can obtain the expression for the indifference location S_i as

$$S_i = \begin{cases} \dfrac{D_i + D_{i+1}}{2} + \dfrac{1}{2(c^R + \alpha_1 t_0^R)}\left(\dfrac{\alpha_2 Q_{i+1}}{K_{i+1}} - \dfrac{\alpha_2 Q_i}{K_i} + (p_{i+1} + \alpha_3\lambda_0 V_{i+1}^{-\lambda_1})D_{i+1} - (p_i + \alpha_3\lambda_0 V_i^{-\lambda_1})D_i\right), & i = 0,1,2,\cdots,N-1, \\ D_N + \dfrac{b - (p_N + \alpha_3\lambda_0 V_N^{-\lambda_1})D_N}{(c^R + \alpha_1 t_0^R)} - \dfrac{\alpha_2 Q_N}{(c^R + \alpha_1 t_0^R)K_N}, & i = N. \end{cases} \quad (9)$$

Let L_i be the length of port *i*'s catchment area $[S_{i-1}, S_i]$, i.e., $L_i = S_i - S_{i-1}$. It is given as

$$L_i = \begin{cases} \dfrac{D_{i+1} - D_{i-1}}{2} + \dfrac{1}{2(c^R + \alpha_1 t_0^R)} \left(\dfrac{\alpha_2 Q_{i+1}}{K_{i+1}} - \dfrac{2\alpha_2 Q_i}{K_i} + \dfrac{\alpha_2 Q_{i-1}}{K_{i-1}} + (p_{i+1} + \alpha_3 \lambda_0 V_{i+1}^{-\lambda_1}) D_{i+1} \right. \\ \left. -2(p_i + \alpha_3 \lambda_0 V_i^{-\lambda_1}) D_i + (p_{i-1} + \alpha_3 \lambda_0 V_{i-1}^{-\lambda_1}) D_{i-1} \right), \ i = 1, 2, \cdots, N-1, \\ \dfrac{D_N - D_{N-1}}{2} + \dfrac{1}{2(c^R + \alpha_1 t_0^R)} \left(2b - \dfrac{3\alpha_2 Q_N}{K_N} + \dfrac{\alpha_2 Q_{N-1}}{K_{N-1}} - 3(p_N + \alpha_3 \lambda_0 V_N^{-\lambda_1}) D_N + (p_{N-1} + \alpha_3 \lambda_0 V_{N-1}^{-\lambda_1}) D_{N-1} \right), \ i = N. \end{cases} \tag{10}$$

Once the catchment area of each port is determined by Eq. (9), one can then determine the total cargo volume of port *i*, denoted as Q_i, based on Eq. (8), as follows:

$$Q_i = \int_{S_{i-1}}^{D_i} q_i(x) dx + \int_{D_i}^{S_i} q_i(x) dx. \tag{11}$$

Obviously, the expression of Q_i depends on the potential cargo demand distribution $q^0(x)$ and the port congestion (see Eq. (5)). For a general form of $q^0(x)$ and the port congestion case, it is difficult to derive a closed-form expression of Q_i. However, for a special case with a uniformly distributed potential cargo demand (i.e., $q^0(x) = q_0$) and no port congestion, one can derive the analytical expression of Q_i in terms of Eqs. (9), (10) and (11), as follows:

$$Q_i = \frac{q_0 \exp\left(-\xi D_i (p_i + \alpha_3 \lambda_0 V_i^{-\lambda_1})\right)}{\xi (c^R + \alpha_1 t_0^R)} \left(2 - \exp\left(-\xi (c^R + \alpha_1 t_0^R)(D_i - S_{i-1})\right) - \exp\left(-\xi (c^R + \alpha_1 t_0^R)(S_i - D_i)\right)\right), \tag{12}$$

where

$$S_i = \begin{cases} \dfrac{D_i + D_{i+1}}{2} + \dfrac{(p_{i+1} + \alpha_3 \lambda_0 V_{i+1}^{-\lambda_1}) D_{i+1} - (p_i + \alpha_3 \lambda_0 V_i^{-\lambda_1}) D_i}{2(c^R + \alpha_1 t_0^R)}, \ i = 0, 1, 2, \cdots, N-1, \\ D_N + \dfrac{b - (p_N + \alpha_3 \lambda_0 V_N^{-\lambda_1}) D_N}{(c^R + \alpha_1 t_0^R)}, \ i = N. \end{cases} \tag{13}$$

It can easily be shown from Eqs. (12) and (13) that as the ship size V_i increases, the total cargo volumes, Q_i and Q_{i+1}, of port *i* itself and its adjacent upstream port *i*+1 increase, the total cargo volume, Q_{i-1}, of its adjacent downstream port *i*-1 decreases, whereas the total cargo volume for each of the non-adjacent ports does not change.

3.2. Profit maximization problem for carriers

The carriers aim to maximize their own net profit by determining waterway freight rate p_i of one container (or one ton of cargo) per unit of distance, ship size V_i, and number of ships

n_i. Let γ be the average load factor of ships, and ω_i be the number of times that the ship V_i visits port *i* per year (or frequency). Then, the total cargo volume of port *i* per year is $Q_i = \gamma n_i \omega_i V_i$. Hence, once V_i and Q_i are given, n_i can then be immediately determined by $n_i = Q_i / \gamma \omega_i V_i$. Thereby, the carriers actually need to determine the variables p_i and V_i.

Let $\pi_i^{(c)}$ be the net profit of carrier *i*. It is the difference of total revenue minus total ship operating cost and total ship acquisition (or capital) cost. The superscript "c" represents the variables associated with carriers. The ship operating cost generally depends on ship size V_i (Merika et al., 2019). For simplicity, we assume that the ship operating cost per container per unit of distance is a linear decreasing function of ship size V_i, i.e., $f_0 - f_1 V_i$, where f_0 and f_1 are the fixed and variable components of the operating cost per container per unit of distance, respectively. The total ship acquisition (or capital) cost for a ship fleet is a function of ship size V_i and number of ships n_i, i.e., $f_2(V_i) n_i$, where $f_2(V_i)$ is the capital cost per ship, and is assumed to be a linear increasing function of ship size V_i (see Hawdon, 1978), i.e., $f_2 + f_3 V_i$, where f_2 and f_3 are the fixed and variable components of the acquisition (or capital) cost per ship, respectively. The profit maximization problem for the carriers with p_i and V_i as decision variables can then be represented as

$$\max \quad \pi_i^{(c)}(p_i, V_i) = p_i D_i Q_i - \tau_i Q_i - (f_0 - f_1 V_i) D_i Q_i - (f_2 + f_3 V_i) n_i, \tag{14}$$

$$\text{s.t.} \quad V_i \le V_i^{\max}, \tag{15}$$

where the total cargo volume Q_i served by carrier *i* is given by Eq. (11). $p_i D_i$ is the total revenue of carrier *i* carrying one container from port *i* to the destination port, which is paid by the shippers. τ_i is the port service charge per container paid to port operators. The first term on the right-hand side of Eq. (14) is the total revenue, the second term is the total port service charges, the third term is the total ship operating cost, and the last term is the total ship acquisition (capital) cost. Constraint (15) is the upper-bound constraint of ship size, which ensures that the ship size adopted by carrier *i* does not exceed the maximum navigable ship size at port *i* due to the restriction of waterway depth.

From the optimality conditions of the above profit maximization model (14), we have

Lemma 1. (i) Given the ship size V_i, the profit function $\pi_i^{(c)}$ is concave with respect to the waterway freight rate vector $\mathbf{P}=\left(p_j, j=1,2,...,N\right)$, which is given by the following system of equations

$$\begin{cases} 2-\xi(p_jD_j-\tau_j-\delta_j)-\dfrac{4}{4-\exp\left(-\xi(c^R+\alpha_1 t_0^R)(D_j-S_{j-1})\right)-\exp\left(-\xi(c^R+\alpha_1 t_0^R)(S_j-D_j)\right)}=0,\ j=1,2,\cdots,N-1, \\ 2-\xi(p_ND_N-\tau_N-\delta_N)-\dfrac{4+2\exp\left(-\xi(c^R+\alpha_1 t_0^R)(S_N-D_N)\right)}{4-\exp\left(-\xi(c^R+\alpha_1 t_0^R)(D_N-S_{N-1})\right)}=0,\ j=N, \end{cases} \tag{16}$$

where $\delta_j=(f_0-f_1V_j)D_j+\dfrac{1}{\gamma\omega_j}\left(\dfrac{f_2}{V_j}+f_3\right)$.

(ii) Given the waterway freight rate p_i, as the ship size V_i increases, the profit $\pi_i^{(c)}$ increases.

Lemma 1 can be proved by showing that the Hessian matrix $H_N(\pi_i^{(c)})$ of objective function (14) is negative definite with respect to the waterway freight rate p_i and is positive definite with regard to the ship size V_i, respectively (see Appendix B for detailed proof). However, $H_N(\pi_i^{(c)})$ is indefinite with regard to p_i and V_i simultaneously. From item (ii), it can be concluded that Eq. (15) must be a binding constraint, i.e. $V_i=V_i^{\max}$.

3.3. Social welfare maximization problem for port operators

As stated before, the port operators aim to determine the port service charge τ_i and the port capacity K_i so as to maximize the total or local social welfare, depending on the port operating regimes adopted. In this paper, we consider two types of port operating regimes, i.e. the coordinated and independent regimes. For the coordinated regime, all ports along the inland river are operated by the central government, aiming to maximize the total social welfare of the entire inland river system. For the independent regime, each port along the inland river corridor is operated by its local government, with an objective of maximizing the local social welfare of its own port.[4]

The social welfare maximization problem under the coordinated regime with τ_i and K_i as

[4] In the definition of the local social welfare of an independent port, the consumer surplus is for the shippers who uses the service of that port (see, e.g. Xiao et al., 2012; Wang and Zhang, 2018; Wang et al., 2020).

decision variables is expressed as

$$SW^{CO}(\tau_i, K_i) = \max \sum_{i=1}^{N} (\pi_i^{(c)} + \pi_i^{(s)} + \pi_i^{(p)}), \tag{17}$$

where the superscript "*CO*" represents the coordinated regime. The superscripts "*c*", "*s*", and "*p*" represent the variables associated with carriers, shippers, and port operators, respectively. The net profit $\pi_i^{(c)}$ of carrier *i* is given by Eq. (14).

In Eq. (17), $\pi_i^{(s)}$ is the consumer surplus of the shippers choosing port *i* to transport their cargos, and can be calculated by

$$\pi_i^{(s)} = \int_{S_{i-1}}^{S_i} \left(\int_0^{q_i(x)} c_i(q)dq - c_i(x)q_i(x) \right) dx, \ i = 1, 2, \cdots, N, \tag{18}$$

where $c_i(q)$ is the inverse demand function, given by Eq. (8).

Port investment costs consist of two components: port dredging investment cost and port capacity investment cost. The dredging investment cost of waterways between ports is not considered as a component of the port investment cost because the waterway dredging projects are implemented by the central government (instead of the local government) through using national finance (instead of the revenue from the port service charges) (Jiang et al., 2018). The net profit of port operator *i*, denoted as $\pi_i^{(p)}$, can thus be calculated by

$$\pi_i^{(p)}(\tau_i, K_i) = \tau_i Q_i - (\beta_0 + \beta_1 K_i) - (\mu_0 + \mu_1 H_i), \ i = 1, 2, \cdots, N, \tag{19}$$

where H_i is waterway depth of port *i*. β_0 and β_1 are the fixed and variable costs of the port capacity investment, respectively. μ_0 and μ_1 are the fixed and variable costs of the port dredging investment, respectively. Fixed costs are those that do not change with traffic volume, and include for example depreciation and insurance premiums on terminal buildings. Variable costs are those that vary with traffic volume. They include, for example, costs for equipments and labors. For more details about the fixed and variable costs classifications of port investment, see for example Talley (2009). The first term on the right-hand side of Eq. (19) is the total operating revenue of port operator *i*. The second and third terms, respectively, represent the costs of port capacity investment and port dredging investment.

Different from the coordinated regime, the independent regime requires each port operator to maximize its own local social welfare by determining the port service charge τ_i and the port

capacity K_i, expressed as

$$SW_i^{ID}(\tau_i, K_i) = \max\ \pi_i^{(c)} + \pi_i^{(s)} + \pi_i^{(p)}, \tag{20}$$

where the superscript "*ID*" represents the independent regime. $\pi_i^{(c)}$, $\pi_i^{(s)}$, and $\pi_i^{(p)}$ are given by Eqs. (14), (18), and (19), respectively.

4. A special case with uniform demand distribution and no port congestion

It is difficult to analyze the solution properties of the models with a general cargo demand distribution function, as presented in the previous section. In this section, we discuss a special case with a uniform cargo demand distribution ($q_i(x) = q_0$) and no port congestion. Particularly, we focus on the cases of "$N = 2$" and/or "$N = 3$" so as to obtain some managerial insights through deriving closed-form solutions. It is expected that the solutions for the special case can serve as a reference or bound of the solutions for a general case with any cargo demand distribution, any number of ports and port congestion.

4.1. Watershed location and port hinterland area

Under the assumption of the uniform cargo demand distribution ($q_i(x) = q_0$), for the case of $N = 3$, we can derive the indifference location $S_i, i = 0,1,2,3$, in terms of Eq. (9), as follows.

$$\begin{cases}
S_0 = \rho\begin{pmatrix} b(\alpha_2 q_0)^3 + 2(\alpha_2 q_0)^3(c^R + \alpha_1 t_0^R)(D_1 + D_2 + D_3) + (\alpha_2 q_0)^2(c^R + \alpha_1 t_0^R)^2\left((5K_1 + 6K_2 + 2K_3)D_1 + (3K_2 + 2K_3)D_2 + K_3 D_3\right) \\ +\alpha_2 q_0(c^R + \alpha_1 t_0^R)^3\left((6K_1K_2 + 4K_1K_3 + 4K_2K_3)D_1 + 2K_2K_3D_2\right) + 4(c^R + \alpha_1 t_0^R)^3 K_1K_2K_3(c^R + \alpha_1 t_0^R + p_1)D_1 \\ +(\alpha_2 q_0)^2(c^R + \alpha_1 t_0^R)(5K_1D_1p_1 + 3K_2D_2p_2 + K_3D_3p_3) + 2\alpha_2 q_0(c^R + \alpha_1 t_0^R)^2\left((3K_2 + 2K_3)K_1D_1p_1 + K_2K_3D_2p_2\right) \end{pmatrix}, \\
S_1 = \rho\begin{pmatrix} 4(c^R + \alpha_1 t_0^R)^3 K_1K_2K_3\left((c^R + \alpha_1 t_0^R)(D_1 + D_2) - D_1p_1 + D_2p_2\right) \\ +b(\alpha_2 q_0)^2\left(\alpha_2 q_0 + 2(c^R + \alpha_1 t_0^R)K_1\right) + 2(\alpha_2 q_0)^3(c^R + \alpha_1 t_0^R)(D_1 + D_2 + D_3) \\ +(\alpha_2 q_0)^2(c^R + \alpha_1 t_0^R)^2\left(2(K_1 + 3K_2 + K_3)D_1 + (4K_1 + 3K_2 + 2K_3)D_2 + (4K_1 + K_3)D_3\right) \\ +\alpha_2 q_0(c^R + \alpha_1 t_0^R)^3\left((6K_1K_2 + 2K_1K_3 + 4K_2K_3)D_1 + (6K_1K_2 + 4K_1K_3 + 2K_2K_3)D_2 + 2K_1K_3D_3\right) \\ +(\alpha_2 q_0)^2(c^R + \alpha_1 t_0^R)(-2K_1D_1p_1 + 3K_2D_2p_2 + K_3D_3p_3) + 2\alpha_2 q_0(c^R + \alpha_1 t_0^R)^2\left(-(3K_2 + K_3)K_1D_1p_1 + (3K_1 + K_3)K_2D_2p_2 + K_1K_3D_3p_3\right) \end{pmatrix}, \\
S_2 = \rho\begin{pmatrix} 2\alpha_2 q_0(c^R + \alpha_1 t_0^R)^2\left(-K_1K_3D_1p_1 - 2(K_1 + K_3)K_2D_2p_2 + 2(K_1 + 2K_2)K_3D_3p_3\right) \\ +(\alpha_2 q_0)^2(c^R + \alpha_1 t_0^R)^2\left(2(K_1 + K_3)D_1 + 2(2K_1 + 2K_2 + K_3)D_2 + (4K_1 + 8K_2 + K_3)D_3\right) \\ +\alpha_2 q_0(c^R + \alpha_1 t_0^R)^3\left(2K_1K_3D_1 + 4(K_1K_2 + K_1K_3 + K_2K_3)D_2 + 2(4K_1K_2 + K_1K_3 + 2K_2K_3)D_3\right) \\ +b(\alpha_2 q_0)^2\left(\alpha_2 q_0 + 2(c^R + \alpha_1 t_0^R)(K_1 + 2K_2)\right) + 4b\alpha_2 q_0(c^R + \alpha_1 t_0^R)^2 K_1K_2 + 2(\alpha_2 q_0)^3(c^R + \alpha_1 t_0^R)(D_1 + D_2 + D_3) \\ +4(c^R + \alpha_1 t_0^R)^3 K_1K_2K_3\left((c^R + \alpha_1 t_0^R)(D_2 + D_3) - D_2p_2 + D_3p_3\right) + (\alpha_2 q_0)^2(c^R + \alpha_1 t_0^R)(-2K_1D_1p_1 - 4K_2D_2p_2 + K_3D_3p_3) \end{pmatrix}, \\
S_3 = \rho\begin{pmatrix} 4b\alpha_2 q_0(c^R + \alpha_1 t_0^R)^2(K_1K_2 + 2K_1K_3 + 2K_2K_3) + 2(\alpha_2 q_0)^3(c^R + \alpha_1 t_0^R)(D_1 + D_2 + D_3) \\ +8(c^R + \alpha_1 t_0^R)^3 K_1K_2K_3\left(b + (c^R + \alpha_1 t_0^R)D_3 - D_3p_3\right) + (\alpha_2 q_0)^2(c^R + \alpha_1 t_0^R)(-2K_1D_1p_1 - 4K_2D_2p_2 - 6K_3D_3p_3) \\ +4\alpha_2 q_0(c^R + \alpha_1 t_0^R)^3\left(K_1K_2D_2 + 2(K_1K_2 + K_1K_3 + K_2K_3)D_3\right) + 4\alpha_2 q_0(c^R + \alpha_1 t_0^R)^2\left(-K_1K_2D_2p_2 - 2(K_1 + K_2)K_3D_3p_3\right) \\ +b(\alpha_2 q_0)^2\left(\alpha_2 q_0 + 2(c^R + \alpha_1 t_0^R)(K_1 + 2K_2 + 3K_3)\right) + (\alpha_2 q_0)^2(c^R + \alpha_1 t_0^R)^2\left(2K_1D_1 + 4(K_1 + K_2)D_2 + 2(2K_1 + 4K_2 + 3K_3)D_3\right) \end{pmatrix},
\end{cases} \tag{21}$$

where

$$\rho=\left(7(\alpha_2 q_0)^3(c^R+\alpha_1 t_0^R)+2(\alpha_2 q_0)^2(c^R+\alpha_1 t_0^R)^2(5K_1+6K_2+3K_3)+4\alpha_2 q_0(c^R+\alpha_1 t_0^R)^3(3K_1K_2+2K_1K_3+2K_2K_3)+8K_1K_2K_3(c^R+\alpha_1 t_0^R)^4\right)^{-1}. \quad (22)$$

The catchment area $L_i, i=1,2,3$ for $N=3$ in terms of Eq. (10) can be expressed as

$$\begin{cases} L_1=\rho\begin{pmatrix} 2b(\alpha_2 q_0)^2(c^R+\alpha_1 t_0^R)K_1+2\alpha_2 q_0(c^R+\alpha_1 t_0^R)^3\left(-K_3D_1+(3K_2+2K_3)D_2+K_3D_3\right)K_1 \\ +(\alpha_2 q_0)^2(c^R+\alpha_1 t_0^R)^2(-3D_1+4D_2+4D_3)K_1-7(\alpha_2 q_0)^2(c^R+\alpha_1 t_0^R)K_1D_1p_1 \\ +4(c^R+\alpha_1 t_0^R)^3K_1K_2K_3\left((c^R+\alpha_1 t_0^R)D_2-2D_1p_1+D_2p_2\right) \\ +2\alpha_2 q_0(c^R+\alpha_1 t_0^R)^2\left(-3(2K_2+K_3)D_1p_1+3K_2D_2p_2+K_3D_3p_3\right)K_1 \end{pmatrix}, \\ L_2=\rho\begin{pmatrix} 4b(\alpha_2 q_0)^2(c^R+\alpha_1 t_0^R)K_2+4b\alpha_2 q_0(c^R+\alpha_1 t_0^R)^2K_1K_2+(\alpha_2 q_0)^2(c^R+\alpha_1 t_0^R)^2(-6D_1+D_2+8D_3)K_2 \\ +2\alpha_2 q_0(c^R+\alpha_1 t_0^R)^3\left(-(3K_1+2K_3)D_1+(-K_1+K_3)D_2+2(2K_1+K_3)D_3\right)K_2 \\ +4(c^R+\alpha_1 t_0^R)^3K_1K_2K_3\left((c^R+\alpha_1 t_0^R)(-D_1+D_3)+D_1p_1-2D_2p_2+D_3p_3\right) \\ -7(\alpha_2 q_0)^2(c^R+\alpha_1 t_0^R)K_2D_2p_2+2\alpha_2 q_0(c^R+\alpha_1 t_0^R)^2\left(3K_1K_2D_1p_1-(5K_1+3K_3)K_2D_2p_2+(K_1+4K_2)K_3D_3p_3\right) \end{pmatrix}, \\ L_3=\rho\begin{pmatrix} 6b(\alpha_2 q_0)^2(c^R+\alpha_1 t_0^R)K_3+8b\alpha_2 q_0(c^R+\alpha_1 t_0^R)^2(K_1+K_2)K_3 \\ +(\alpha_2 q_0)^2(c^R+\alpha_1 t_0^R)^2(-2D_1-2D_2+5D_3)K_3-7(\alpha_2 q_0)^2(c^R+\alpha_1 t_0^R)K_3D_3p_3 \\ +2\alpha_2 q_0(c^R+\alpha_1 t_0^R)^3\left(-K_1D_1-2(K_1+K_2)D_2+(3K_1+2K_2)D_3\right)K_3 \\ +2\alpha_2 q_0(c^R+\alpha_1 t_0^R)^2\left(K_1D_1p_1+2K_2D_2p_2-2(3K_1+4K_2)D_3p_3\right)K_3 \\ +(c^R+\alpha_1 t_0^R)^3K_1K_2K_3\left(8b+4(c^R+\alpha_1 t_0^R)(-D_2+D_3)+4D_2p_2-12D_3p_3\right) \end{pmatrix}. \end{cases} \quad (23)$$

In order to look at the effects of the waterway/road freight rate p_i on the indifference location S_i and the catchment area L_i, we carry out comparative statics analyses of S_i and L_i with regard to p_i and c^R for the uniformly distributed cargo demand case (i.e., $q_i(x)=q_0$) with N = 3. The comparative statics results are summarized in Table 2. The associated properties are formulated as follows, with detailed proofs given in Appendix C.

Table 2 Comparative statics results of S_i and L_i with regard to p_i and c^R.

	S_0	S_1	S_2	S_3	L_1	L_2	L_3
p_1	+	—	—	—	—	+	+
p_2	+	+	—	—	+	—	+
p_3	+	+	+	—	+	+	—
c^R	—	Undetermined		—	Undetermined		

Note: "+" means a positive correlation and "—" means a negative correlation.

Proposition 1. For the uniformly distributed cargo demand case with N = 3, we have

(i) As the waterway freight rate p_i per unit of distance increases, the watershed location S_j of any port j ($j \geq i$) moves towards port j, while the watershed location S_j of any port j ($j < i$) moves towards port j+1; the catchment area L_i of port i itself decreases, while the

catchment areas of all other ports increase.

(ii) As the road freight rate c^R per unit of distance increases, the watershed locations, S_0 and S_3, of ports 0 and 3 move towards adjacent downstream ports. However, the changes of the other watershed locations S_1 and S_2 and the catchment areas of ports 1, 2, 3 are ambiguous.

Item (i) of Proposition 1 shows that as the waterway freight rate p_i of port *i* increases, its hinterland area reduces (i.e., $\partial L_i/\partial p_i < 0$, see Eqs. (C.4)-(C.6)), whereas the hinterland areas of all other ports (including non-adjacent ports) enlarge ($\partial L_j/\partial p_i > 0, j \neq i$). As a result, the cargo demand of port *i* decreases, whereas the cargo demands of all other ports increase. Item (ii) shows that as c^R increases, S_0 and S_3 decrease in terms of $\partial S_0/\partial c^R < 0$ and $\partial S_3/\partial c^R < 0$ in Eq. (C.7), meaning that S_0 and S_3 move towards ports 0 and 3, respectively. However, for S_1 and S_2, owing to a competition between adjacent ports *i* and *i*+1 for the inland market $(D_i, D_{i+1}), i = 1,2$, a change of $S_i, i = 1,2$ depends on the waterway freight rates of ports *i* and *i*+1, leading the sign of $\partial S_i/\partial c^R, i = 1,2$ to be ambiguous. If $\partial S_i/\partial c^R < 0, i = 1,2$ holds, then port *i*+1 has a bigger market power than port *i* due to a decrease in S_i. This means that as c^R increases, port *i* loses some upstream hinterland area.

4.2. Profit maximization for carriers

As previously shown, the optimal solution of the ship size V_i for a general case must take its boundary value, i.e., $V_i = V_i^{\max}$. Hence, one only needs to determine the optimal waterway freight rate solution p_i for the carriers. In order to derive the optimal solution p_i for the case with uniform cargo demand distribution ($q_i(x) = q_0$) and no port congestion, we set the partial derivative of objective function $\pi_i^{(c)}$ in Eq. (14) with respect to p_i as zero. For $N = 2$, one can derive the analytical solutions of the waterway freight rates $p=(p_1, p_2)$ of ports 1 and 2 as

$$\begin{cases} p_1 = \dfrac{(c^R + \alpha_1 t_0^R)(-D_1 + 7D_2) + 12(\tau_1 + \delta_1) + 3(\tau_2 + \delta_2) + \alpha_3(-11t_1D_1 + 3t_2D_2) + 2b}{23D_1}, \\ p_2 = \dfrac{(c^R + \alpha_1 t_0^R)(-4D_1 + 5D_2) + 2(\tau_1 + \delta_1) + 12(\tau_2 + \delta_2) + \alpha_3(2t_1D_1 - 11t_2D_2) + 8b}{23D_2}, \end{cases} \tag{24}$$

where t_i is given by Eq. (3).

For $N = 3$, one can derive the analytical solutions of the waterway freight rates $p=(p_1, p_2, p_3)$ of ports 1, 2, and 3 as

$$\begin{cases} p_1 = \dfrac{(c^R + \alpha_1 t_0^R)(-6D_1 + 22D_2 + 7D_3) + 46(\tau_1 + \delta_1) + 12(\tau_2 + \delta_2) + 3(\tau_3 + \delta_3) + \alpha_3(-40t_1D_1 + 12t_2D_2 + 3t_3D_3) + 2b}{86D_1}, \\ p_2 = \dfrac{(c^R + \alpha_1 t_0^R)(-12D_1 + D_2 + 14D_3) + 6(\tau_1 + \delta_1) + 24(\tau_2 + \delta_2) + 6(\tau_3 + \delta_3) + \alpha_3(6t_1D_1 - 19t_2D_2 + 6t_3D_3) + 4b}{43D_2}, \\ p_3 = \dfrac{(c^R + \alpha_1 t_0^R)(-4D_1 - 14D_2 + 19D_3) + 2(\tau_1 + \delta_1) + 8(\tau_2 + \delta_2) + 45(\tau_3 + \delta_3) + \alpha_3(2t_1D_1 + 8t_2D_2 - 41t_3D_3) + 30b}{86D_3}. \end{cases} \tag{25}$$

From Eqs. (24) and (25), one can identify the impacts of the port service charge τ_i on the waterway freight rate p_i, as follows. The detailed proofs are given in Appendix D.

Proposition 2. For the special case with a uniformly distributed cargo demand and no port congestion, it can be shown that

(i) Increasing the service charge of port *i* leads to an increase in the waterway freight rates of carriers of all ports. The marginal effect of the service charge of port *i* on the freight rate of port *i* itself is largest, on the adjacent port is second largest, and on the non-adjacent port is smallest;

(ii) The marginal effect of the service charge of the upstream port on the waterway freight rate of the downstream carrier is always not less than the marginal effect of the service charge of the downstream port on the waterway freight rate of the upstream carrier.

The economic implications of Proposition 2 are explained as follows. In item (i), an increase in the service charge of a port means that the carrier using that port has to pay more money to the associated port operator. In order to increase its net profit, the carrier intends to increase its waterway freight rate, which is paid by the shippers. As a result, the carriers using other ports also increase their waterway freight rates due to the complementary relationship between the variables p_i and p_j ($i \neq j$) in the port game (Wan et al., 2016), i.e., one of them increases, then the other also increase, and vice versa. However, such interrelated effects

are marginally decreasing with an increase in the distance between ports. As for item (ii), as the port service charge of an upstream port increases, the waterway freight rate of the carrier of that port increases, thus leading to a reduced hinterland area of that port due to transfer of some cargos to the adjacent upstream and downstream ports. As a result, the hinterland areas of the upstream and downstream ports increase. However, the increased hinterland area of the downstream port is larger than that of the upstream port because the downstream port is closer to the destination port than the upstream port, meaning a lower waterway transport cost under no congestion condition. Thereby, the change of the waterway freight rate of the downstream carrier is greater than that of the upstream carrier.

It should be pointed out that for other potential cargo demand distributions, the analytical solutions of the waterway freight rate p_i and the solution properties of the model are not derived due to difficulty in mathematical tractability. In the illustrative example followed, an example with a linear potential cargo demand distribution will be numerically explored.

4.3. Social welfare maximization for port operators

4.3.1. Optimal port service charge

From the first-order optimality condition of maximization problems (17) and (20), one can derive the optimal port service charges τ_i^{CO} and τ_i^{ID} under the coordinated and independent regimes, respectively. For $N = 2$, we have

$$\begin{cases} \tau_1^{CO} = \dfrac{(c^R + \alpha_1 t_0^R)(-2D_1 + 3D_2) - 5(\delta_2 + \alpha_3 t_2 D_2) + 4b}{20}, \\ \tau_2^{CO} = \dfrac{(c^R + \alpha_1 t_0^R)(-3D_1 + 13D_2) - 17(\delta_1 + \alpha_3 t_1 D_1) + 7b}{100}, \end{cases} \tag{26}$$

$$\begin{cases} \tau_1^{ID} = \dfrac{(c^R + \alpha_1 t_0^R)(-4D_1 + 27D_2) - 42(\delta_1 + \alpha_3 t_1 D_1) + 11(\delta_2 + \alpha_3 t_2 D_2) + 8b}{1000}, \\ \tau_2^{ID} = \dfrac{(c^R + \alpha_1 t_0^R)(-66D_1 + 6D_2 + 78D_3) + 7(\delta_1 + \alpha_3 t_1 D_1) - 42(\delta_2 + \alpha_3 t_2 D_2) + 30b}{1000}, \end{cases} \tag{27}$$

where $\delta_i = (f_0 - f_1 \eta H_i) D_i + \dfrac{1}{\gamma \omega_i} \left(\dfrac{f_2}{\eta H_i} + f_3 \right)$.

For $N = 3$, one can derive

$$\begin{cases} \tau_1^{CO} = \dfrac{(c^R + \alpha_1 t_0^R)(-21D_1 + 4D_2 + 29D_3) - 25(\delta_2 + \alpha_3 t_2 D_2) + 14b}{100}, \\ \tau_2^{CO} = \dfrac{(c^R + \alpha_1 t_0^R)(-18D_1 + 7D_2 + 32D_3) - 25(\delta_1 + \alpha_3 t_1 D_1 + \delta_3 + \alpha_3 t_3 D_3) + 29b}{100}, \\ \tau_3^{CO} = \dfrac{(c^R + \alpha_1 t_0^R)(-14D_1 + 2D_2 + 19D_3) - 17(\delta_2 + \alpha_3 t_2 D_2) + 10b}{100}. \end{cases} \tag{28}$$

$$\begin{cases} \tau_1^{ID} = \dfrac{(c^R + \alpha_1 t_0^R)(-11D_1 + 39D_2 + 13D_3) - 65(\delta_1 + \alpha_3 t_1 D_1) + 18(\delta_2 + \alpha_3 t_2 D_2) + 5(\delta_3 + \alpha_3 t_3 D_3) + 4b}{1000}, \\ \tau_2^{ID} = \dfrac{(c^R + \alpha_1 t_0^R)(-66D_1 + 6D_2 + 78D_3) + 31(\delta_1 + \alpha_3 t_1 D_1) - 100(\delta_2 + \alpha_3 t_2 D_2) + 32(\delta_3 + \alpha_3 t_3 D_3) + 23b}{1000}, \\ \tau_3^{ID} = \dfrac{(c^R + \alpha_1 t_0^R)(-5D_1 - 15D_2 + 21D_3) + 2(\delta_1 + \alpha_3 t_1 D_1) + 8(\delta_2 + \alpha_3 t_2 D_2) - 44(\delta_3 + \alpha_3 t_3 D_3) + 33b}{1000}. \end{cases} \tag{29}$$

From Eqs. (26)-(29), one can immediately obtain the following proposition, which reveals the relationships between the port service charge and the waterway depth under different port operating regimes. The proof is given in Appendix E.

Proposition 3. (i) Under the coordinated regime, as port *i*'s waterway depth H_i increases, the service charges τ_j^{CO} (j = i–1, i+1) of port *i*'s adjacent ports (including downstream and upstream ports) increase, whereas the service charges of port *i* itself and its non-adjacent ports do not change;

(ii) Under the independent regime, as port *i*'s waterway depth H_i increases, the service charge τ_i^{ID} of port *i* itself increases, but the service charges τ_j^{ID} ($j \neq i$) of other competitive ports decrease. Increasing the waterway depth of other port *j* ($j \neq i$) leads to a decrease in the service charge of port *i*.

Proposition 3 shows that the port operating regimes lead to distinct properties, in terms of the effects of the waterway depth on the port service charges of port operators. Specifically, item (i) implies that under the central government's regulation, the adjacent ports' charges increase in response to one port's increase in waterway depth. This is because the government wants to discourage the shippers to use the adjacent ports and better utilize the benefit of the waterway depth increase (larger ship and economies of scale). However, the service charges of farther non-adjacent ports and port itself are not affected. Item (ii) means that under the local government's respective regulation, increasing the waterway depth of a port can shorten the average transport time of cargos of that port and thus improve its attractiveness. As a result, its service charge increases due to improved service, while the service charges of other

competitive ports decrease due to lowered attractiveness.

As a byproduct, substituting Eqs. (26)-(29) into Eqs. (24) and (25), one can further represent the optimal waterway freight rate solutions p_i^{CO} and p_i^{ID} of the carriers under the coordinated and independent regimes as follows. For $N = 2$, we have

$$\begin{cases} p_1^{CO} = \dfrac{(c^R + \alpha_1 t_0^R)(-2D_1 + 9D_2) + 12\delta_1 - 11\alpha_3 t_1 D_1 + 5b}{25D_1}, \\ p_2^{CO} = \dfrac{(c^R + \alpha_1 t_0^R)(-5D_1 + 7D_2) + 0.01(\delta_1 + \alpha_3 t_1 D_1) + 12(\delta_2 - \alpha_3 t_2 D_2) + 9b}{25D_2}. \end{cases} \tag{30}$$

$$\begin{cases} p_1^{ID} = \dfrac{(c^R + \alpha_1 t_0^R)(-D_1 + 7D_2) + (12\delta_1 - 11\alpha_3 t_1 D_1) + 3(\delta_2 + \alpha_3 t_2 D_2) + 2b}{25D_1}, \\ p_2^{ID} = \dfrac{(c^R + \alpha_1 t_0^R)(-4D_1 + 5D_2) + 2(\delta_1 + \alpha_3 t_1 D_1) + (12\delta_2 - 11\alpha_3 t_2 D_2) + 8b}{25D_2}. \end{cases} \tag{31}$$

For $N = 3$, we have

$$\begin{cases} p_1^{CO} = \dfrac{(c^R + \alpha_1 t_0^R)(-18D_1 + 25D_2 + 25D_3) + 43(\delta_1 - \alpha_3 t_1 D_1) + 0.03(\delta_2 + \alpha_3 t_2 D_2) + 12b}{100D_1}, \\ p_2^{CO} = \dfrac{(c^R + \alpha_1 t_0^R)(-18D_1 + 3D_2 + 25D_3) + (22\delta_2 - 21\alpha_3 t_2 D_2) + 12b}{50D_2}, \\ p_3^{CO} = \dfrac{(c^R + \alpha_1 t_0^R)(-12D_1 - 12D_2 + 31D_3) + 0.04(\delta_2 + \alpha_3 t_2 D_2) + 43(\delta_3 - \alpha_3 t_3 D_3) + 37b}{100D_3}. \end{cases} \tag{32}$$

$$\begin{cases} p_1^{ID} = \dfrac{(c^R + \alpha_1 t_0^R)(-7D_1 + 24D_2 + 9D_3) + 43(\delta_1 - \alpha_3 t_1 D_1) + 12(\delta_2 + \alpha_3 t_2 D_2) + 4(\delta_3 + \alpha_3 t_3 D_3) + 3b}{100D_1}, \\ p_2^{ID} = \dfrac{(c^R + \alpha_1 t_0^R)(-14D_1 + D_2 + 16D_3) + 6(\delta_1 + \alpha_3 t_1 D_1) + (22\delta_2 - 21\alpha_3 t_2 D_2) + 7(\delta_3 + \alpha_3 t_3 D_3) + 5b}{50D_2}, \\ p_3^{ID} = \dfrac{(c^R + \alpha_1 t_0^R)(-5D_1 - 15D_2 + 21D_3) + 2(\delta_1 + \alpha_3 t_1 D_1) + 8(\delta_2 + \alpha_3 t_2 D_2) + 43(\delta_3 - \alpha_3 t_3 D_3) + 32b}{100D_3}. \end{cases} \tag{33}$$

From Eqs. (30)-(33), the relationships between the waterway freight rate and the waterway depth under two port operating regimes are as follows. Its proof is given in Appendix F.

Proposition 4. (i) Under the coordinated regime, changing the waterway depth of port i, H_i, has trivial effects on the waterway freight rates of other ports, but has an ambiguous effect on the waterway freight rate of that port itself, depending on the sign of $\dfrac{D_i f_1 \gamma \omega_i (\eta H_i)^2 + f_2}{D_i \alpha_3 \lambda_0 \lambda_1 \gamma \omega_i (\eta H_i)^{1-\lambda_1}}$.

(ii) Under the independent regime, as port i's waterway depth H_i increases, the waterway

freight rates p_j^{ID} ($j \neq i$) of other competitive ports decrease, while the change of the waterway freight rate p_i^{ID} of port i itself is ambiguous, depending on the sign of $\frac{D_i f_1 \gamma \omega_i (\eta H_i)^2 + f_2}{D_i \alpha_3 \lambda_0 \lambda_1 \gamma \omega_i (\eta H_i)^{1-\lambda_1}}$. Increasing the waterway depths of other ports leads to a decrease in the freight rate of port i.

Proposition 4 further shows that there is a significant difference between different port operating regimes, in terms of the effects of the waterway depth on the waterway freight rates of carriers. Specifically, item (i) means that under the central government's regulation, the effects of the waterway depth on the waterway freight rates of other ports are very weak and can be neglected, whereas the effects on the waterway freight rate of that port itself are significant. Item (ii) shows that under the local government's respective regulation, changing the waterway depth of a port affects the freight rates of all ports.

4.3.2. Maximum social welfare

Substituting Eqs. (30)-(33) into Eqs. (17) and (20), one can obtain the maximum social welfare of each port under the coordinated (SW_i^{CO}) and independent (SW_i^{ID}) regimes. For N = 2, we have

$$\begin{cases} SW_1^{CO} = \dfrac{q_0(p_1^{CO}D_1 - \delta_1)}{50(c^R + \alpha_1 t_0^R)} \begin{pmatrix} (c^R + \alpha_1 t_0^R)(-D_1 + 14D_2) - (24\delta_1 + 25\alpha_3 t_1 D_1) \\ +(12\delta_2 + 13\alpha_3 t_2 D_2) - b \end{pmatrix} - (\mu_0 + \mu_1 H_1) - (\beta_0 + \beta_1 K_1), \\ SW_2^{CO} = \dfrac{q_0(p_2^{CO}D_2 - \delta_2)}{50(c^R + \alpha_1 t_0^R)} \begin{pmatrix} (c^R + \alpha_1 t_0^R)(-12D_1 + 13D_2) + 2(6\delta_1 + 7\alpha_3 t_1 D_1) \\ -3(12\delta_2 + 13\alpha_3 t_2 D_2) + 28b \end{pmatrix} - (\mu_0 + \mu_1 H_2) - (\beta_0 + \beta_1 K_2). \end{cases} \quad (34)$$

$$\begin{cases} SW_1^{ID} = \dfrac{q_0(p_1^{ID}D_1 - \delta_1)}{50(c^R + \alpha_1 t_0^R)} \begin{pmatrix} (c^R + \alpha_1 t_0^R)(-2D_1 + 16D_2) - 2(11\delta_1 + 13\alpha_3 t_1 D_1) \\ +2(3\delta_2 + 4\alpha_3 t_2 D_2) + 4b \end{pmatrix} - (\mu_0 + \mu_1 H_1) - (\beta_0 + \beta_1 K_1), \\ SW_2^{ID} = \dfrac{q_0(p_2^{ID}D_2 - \delta_2)}{50(c^R + \alpha_1 t_0^R)} \begin{pmatrix} (c^R + \alpha_1 t_0^R)(-24D_1 + 17D_2) + 2(3\delta_1 + 4\alpha_3 t_1 D_1) \\ -3(11\delta_2 + 13\alpha_3 t_2 D_2) + 28b \end{pmatrix} - (\mu_0 + \mu_1 H_2) - (\beta_0 + \beta_1 K_2). \end{cases} \quad (35)$$

For N = 3, we have

$$\begin{cases} SW_1^{CO} = \dfrac{q_0(p_1^{CO}D_1-\delta_1)}{100(c^R+\alpha_1 t_0^R)}\left(78(c^R+\alpha_1 t_0^R)D_2-(43\delta_1+57\alpha_3 t_1 D_1)+(22\delta_2+29\alpha_3 t_2 D_2)\right)-(\mu_0+\mu_1 H_1)-(\beta_0+\beta_1 K_1), \\ SW_2^{CO} = \dfrac{q_0(p_2^{CO}D_2-\delta_2)}{200(c^R+\alpha_1 t_0^R)}\begin{pmatrix}(c^R+\alpha_1 t_0^R)(-58D_1+D_2+56D_3)+(43\delta_1+57\alpha_3 t_1 D_1)\\ -(88\delta_2+116\alpha_3 t_2 D_2)+(43\delta_3+57\alpha_3 t_3 D_3)+b\end{pmatrix}-(\mu_0+\mu_1 H_2)-(\beta_0+\beta_1 K_2), \\ SW_3^{CO} = \dfrac{q_0(p_3^{CO}D_3-\delta_3)}{200(c^R+\alpha_1 t_0^R)}\begin{pmatrix}(c^R+\alpha_1 t_0^R)(-58D_2+57D_3)+2(22\delta_2+29\alpha_3 t_2 D_2)\\ -(129\delta_3+171\alpha_3 t_3 D_3)+113b\end{pmatrix}-(\mu_0+\mu_1 H_3)-(\beta_0+\beta_1 K_3). \end{cases} \tag{36}$$

$$\begin{cases} SW_1^{ID} = \dfrac{q_0(p_1^{ID}D_1-\delta_1)}{100(c^R+\alpha_1 t_0^R)}\begin{pmatrix}(c^R+\alpha_1 t_0^R)(-7D_1+27D_2+7D_3)-(37\delta_1+51\alpha_3 t_1 D_1)\\ +(10\delta_2+17\alpha_3 t_2 D_2)+3(\delta_3+\alpha_3 t_3 D_3)+2b\end{pmatrix}-(\mu_0+\mu_1 H_1)-(\beta_0+\beta_1 K_1), \\ SW_2^{ID} = \dfrac{q_0(p_2^{ID}D_2-\delta_2)}{200(c^R+\alpha_1 t_0^R)}\begin{pmatrix}(c^R+\alpha_1 t_0^R)(-56D_1+5D_2+66D_3)+(21\delta_1+35\alpha_3 t_1 D_1)\\ -(68\delta_2+96\alpha_3 t_2 D_2)+(19\delta_3+33\alpha_3 t_3 D_3)+15b\end{pmatrix}-(\mu_0+\mu_1 H_2)-(\beta_0+\beta_1 K_2), \\ SW_3^{ID} = \dfrac{q_0(p_3^{ID}D_3-\delta_3)}{200(c^R+\alpha_1 t_0^R)}\begin{pmatrix}(c^R+\alpha_1 t_0^R)(-13D_1-53D_2+69D_3)+6(\delta_1+\alpha_3 t_1 D_1)\\ +2(10\delta_2+17\alpha_3 t_2 D_2)-(115\delta_3+157\alpha_3 t_3 D_3)+114b\end{pmatrix}-(\mu_0+\mu_1 H_3)-(\beta_0+\beta_1 K_3). \end{cases} \tag{37}$$

From Eqs. (34)-(37), one can immediately obtain the following proposition, which shows the relationships between the social welfare of each port and the waterway depths under different port operating regimes. Its proof is given in Appendix G.

Proposition 5. (i) Under the coordinated regime, as port *i*'s waterway depth H_i increases, the social welfare SW_i^{CO} of port *i* itself increases, the social welfares SW_j^{CO} ($j = i$-1, i+1) of its adjacent ports (including downstream and upstream ports) decrease, while the social welfare of non-adjacent port does not change.

(ii) Under the independent regime, as port *i*'s waterway depth H_i increases, the social welfare SW_i^{ID} of port *i* itself increases, but the social welfares SW_j^{ID} ($j \neq i$) of other competitive ports decrease.

Proposition 5 further shows that under the central government's regulation, the change of the waterway depth of a port influences the social welfares of its adjacent ports and itself. However, under the local government's respective regulation, changing the waterway depth of a port influences the social welfare of each port in the corridor system.

5. Numerical studies

5.1. Parameter calibrations

In this section, 7 major inland river ports along the Yangtze River of China (i.e., Taicang port, Zhenjiang port, Nanjing port, Wuhu port, Wuhan port, Chongqing port, and Yibin port) are employed to illustrate the properties and applications of the proposed models. The Shanghai port is considered as the destination port, which serves as a key transshipment port and interface between inland shipping and maritime shipping. The distances of the 7 inland river ports from the Shanghai port are 75, 283, 347, 503, 1043, 2329 and 2783 km, respectively, i.e., D = [75, 283, 347, 503, 1043, 2329, 2783] km. Their actual waterway depths are H = [12.5, 12.5, 12.5, 7.5, 4.5, 3.5, 2.9] m, and their capacities are K = [148, 159, 200, 140, 95.02, 96.7, 15] million tons per year.[5] The frequencies that ships visit ports are ω_i = [230, 120, 97, 67, 42, 35, 12] times per year. In practice, one major shipping commodity is containerized cargo, which can be conveniently handled by multi-modal transport systems. However, its handling rates are not routinely and consistently reported by government agencies, and significantly change over time. The commonly available rates are based on weights (i.e. tons). Apparently, if a consistent weight per container is used, the same results will be obtained regardless of cargo units. Because the most readily available data are all at tons, the numerical simulation is weight-based, which yields the same pattern (although not the same number) as container based calculation. The road freight rate of one ton of cargo per unit of distance is set as c^R=RMB0.5/ton-km.[6] Here, "RMB" stands for the Chinese currency "Renminbi". US$1 approximates RMB6.52 as of January 1, 2021. The road transport time per unit of distance is t_0^R=0.01 h/km. The values of road transport time, port congestion delay and waterway transport time perceived by shippers are $\alpha_1 = 5.0$, $\alpha_2 = 3.5$, and $\alpha_3 = 1.0$ (RMB/h/ton-km), respectively. The maximum acceptable full transport cost of shippers per unit of cargo is b = RMB470/ton. The average load factor of ships is γ = 90%. The variable and fixed costs of port capacity investment are β_1 = RMB5.0/ton and β_0 =3.0 million RMB, respectively. The variable and fixed costs of the port dredging investment are μ_1=1.0 million RMB/ton and μ_0 =6.0 million RMB, respectively. Other parameters are: $\lambda_0 = 0.5$, $\lambda_1 = 0.28$, f_0=RMB0.005/ton-km, f_1=RMB2.0×10^{-7}/ton^2-km, f_2=RMB120000, f_3= RMB10/ton, and η=1000 ton/m.

In this example, we consider a linear potential cargo demand density function, specified as

[5] http://www.cjhdj.com.cn/hdfw/ndssjh.

[6] https://wenku.baidu.com/view/813699fd910ef12d2af9e7bd.html.

$$q^0(x) = q_0 + q_1 x, \tag{38}$$

where q_0 is the constant potential cargo demand, and q_1 is the density gradient describing how rapidly the cargo demand density changes with distance *x* from the destination port. As $q_1 = 0$, the linear demand density function is reduced to a uniformly distributed one.

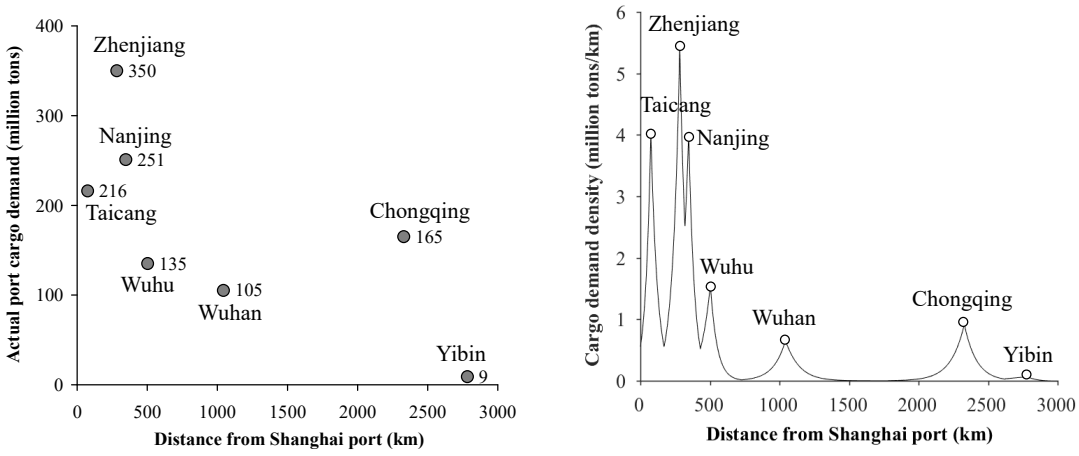

(a) (b)

Fig. 5. (a) Actual port cargo demand in 2020; (b) cargo demand density along the river corridor.

Fig. 5a shows the total actual cargo demand of each port in 2020. Using the actual cargo demand density function (8) and the linear potential cargo demand density function (38), one can derive the expressions for the potential cargo demand density $q^0(x)$, as shown in Eq. (39), which is a piece-wise function consisting of the following segments: Taicang – Zhenjiang, Zhenjiang – Wuhu, Wuhu – Wuhan, Wuhan – Chongqing, and Chongqing – Yibin.[7] It is assumed that the price elasticity of the cargo demand is 1.0, and thus the demand elasticity parameter ξ_i in the cargo demand density function (8) is the reciprocal of actual waterway freight rate, i.e., $\xi_i = 1/(p_i D_i)$, see Tan et al. (2015). Accordingly, in this example the actual cargo demand density function (8) can be further written as Eq. (40), as shown in Fig. 5b. In the following analysis, the afore-described input data and model parameter values are considered to be the base case unless stated otherwise.

[7] The potential cargo demand density functions of Zhenjiang port to Nanjing port and Nanjing port to Wuhu port are approximated as a linear function.

$$q^0(x)=\begin{cases}12059370+42870x,\ x\in[0,283],\\ 41049890-59570x,\ x\in[283,503],\\ 15345081-8467x,\ x\in[503,1043],\\ -14346000+20000x,\ x\in[1043,2329],\\ 158000000-54000x,\ x\in[2329,+\infty].\end{cases} \tag{39}$$

$$q_i(x)=q^0(x)\exp\left(-\xi c_i(x)\right)=\begin{cases}q^0(x)\exp\left(-0.0425c_1(x)\right),\ x\in[S_0,S_1],\ \text{for Taicang},\\ q^0(x)\exp\left(-0.0332c_2(x)\right),\ x\in[S_1,S_2],\ \text{for Zhenjiang},\\ q^0(x)\exp\left(-0.0380c_3(x)\right),\ x\in[S_2,S_3],\ \text{for Nanjing},\\ q^0(x)\exp\left(-0.0360c_4(x)\right),\ x\in[S_3,S_4],\ \text{for Wuhu},\\ q^0(x)\exp\left(-0.0235c_5(x)\right),\ x\in[S_4,S_5],\ \text{for Wuhan},\\ q^0(x)\exp\left(-0.0177c_6(x)\right),\ x\in[S_5,S_6],\ \text{for Chongqing},\\ q^0(x)\exp\left(-0.0165c_7(x)\right),\ x\in[S_6,S_7],\ \text{for Yibin},\end{cases} \tag{40}$$

where the watershed locations $S_i(i=0,1,\cdots,7)$ between ports can be determined by Eq. (9), which are presented later.

5.2. Discussion of results

5.2.1. Comparison of solutions under different port operating regimes

According to Eq. (9), one can determine the watershed locations $S_i(i=0,1,\cdots,7)$ between ports under the coordinated and independent regimes, as shown in Fig. 6. It can be seen in this figure that the resultant hinterland areas of Taicang port (TC), Zhenjiang port (ZJ), Nanjing port (NJ), Wuhu port, Wuhan port, Chongqing port (CQ), and Yibin port (YB) are 126, 123, 117, 378, 970, 861, and 460 (km) for the coordinated regime, and 125, 121, 123, 376, 967, 856, and 475 (km) for the independent regime, respectively. Compared to the coordinated regime, the independent regime can cause a slight decrease in the hinterland areas of all ports, except for Nanjing port and Yibin port. This is because the full transport cost under the independent regime is much less than that under the coordinated regime for the port pairs of Nanjing-Shanghai and Yibin-Shanghai (over RMB5.0/ton), as shown in Table 3. Thereby, the attractiveness of Nanjing and Yibin ports and thus market powers are stronger under the independent regime. In other words, as the full transport cost of a port with the independent regime decreases to a certain extent compared to the coordinated regime (e.g., Nanjing and Yibin ports), the hinterland area of that port with the independent regime is larger than that with the coordinated regime. It can also be seen that the whole service coverage of the river

corridor under the independent regime is 8 km (from 3035 to 3043 km) bigger than that under the coordinated regime. This is attributed to the competition between the local governments for hinterland cargo demand under the independent regime so as to maximize their own local social welfare.

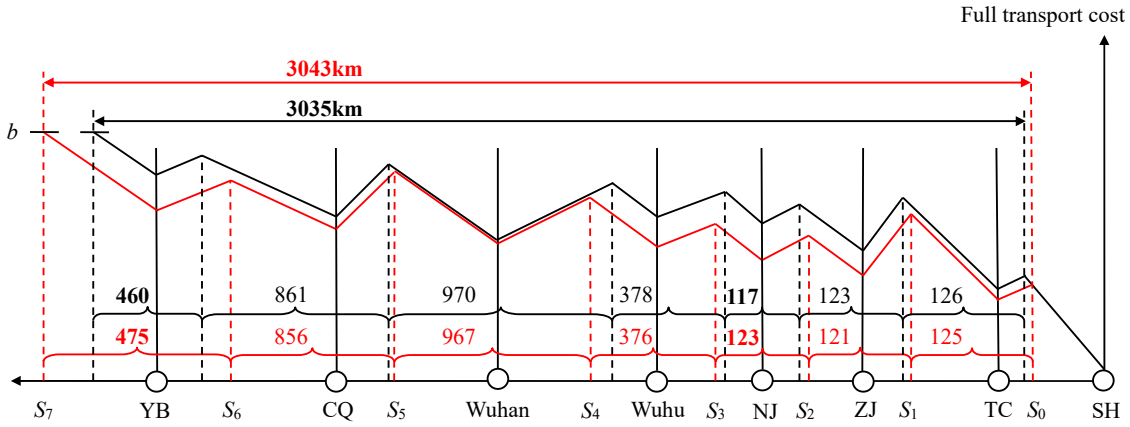

Fig. 6. Catchment area of each inland river port under coordinated (in black) and independent (in red) regimes.

Table 3 Full transport costs of port pairs under coordinated and independent regimes.

Port pair	Coordinated (RMB/ton)	Independent (RMB/ton)	Change (RMB/ton)
Taicang-Shanghai	32.27	31.25	1.03
Zhenjiang-Shanghai	47.57	44.92	2.65
Nanjing-Shanghai	47.87	42.57	5.30
Wuhu-Shanghai	56.42	54.42	2.00
Wuhan-Shanghai	97.90	97.82	0.08
Chongqing-Shanghai	201.55	201.06	0.49
Yibin-Shanghai	295.09	289.44	5.66

Note: Change = coordinated – independent.

Table 4 summaries the results of the optimal decisions of carriers and port operators under the coordinated and independent regimes. It can be noted that the relative changes of the cargo volume, each carrier's profit and each port's consumer surplus for all ports are negative. This means that in comparison with the coordinated regime, the independent regime can cause an increase in the cargo volume, carrier's profit and port's consumer surplus for each port due to a lower waterway freight rate under the independent regime. Particularly, the relative change of Nanjing port is largest (>20%), that of Yibin port is second largest (about 10%), and those of Wuhan and Chongqing ports are smallest (<1%). This implies that the operating regimes have a significant effect on the Nanjing and Yibin ports because of their significantly

decreased full transport costs under the independent regime, and such an effect is small for other ports. It can also be noted that the relative changes of the social welfares of all ports are positive, except for Nanjing port and Yibin port. This means that the independent regime is superior to the coordinated regime for Nanjing and Yibin ports (two ports with full transport costs significantly decreased), in terms of individual local social welfare.

Table 4 Results under coordinated and independent regimes.

Performance index	Inland river port	Coordinated	Independent	Relative change (%)
Cargo demand (million tons)	Taicang	198.89	210.26	-5.41
	Zhenjiang	324.59	348.87	-6.96
	Nanjing	199.80	251.16	-20.45
	Wuhu	133.75	142.10	-5.88
	Wuhan	114.54	114.68	-0.12
	Chongqing	163.25	164.58	-0.81
	Yibin	8.81	9.80	-10.04
	Total	1143.62	1241.45	-7.88
Carrier's profit (million RMB)	Taicang	4353.81	4680.15	-6.97
	Zhenjiang	9974.84	10825.63	-7.86
	Nanjing	4861.00	6423.11	-24.32
	Wuhu	3842.80	4094.04	-6.14
	Wuhan	5288.53	5294.12	-0.11
	Chongqing	10119.70	10206.53	-0.85
	Yibin	481.41	539.63	-10.79
	Total	38922.09	42063.21	-7.47
Consumer surplus (million RMB)	Taicang	4679.69	4947.20	-5.41
	Zhenjiang	9776.79	10508.11	-6.96
	Nanjing	5257.79	6609.54	-20.45
	Wuhu	3715.16	3947.23	-5.88
	Wuhan	4874.03	4880.00	-0.12
	Chongqing	9222.98	9298.33	-0.81
	Yibin	534.12	593.72	-10.04
	Total	38060.56	40784.14	-6.68
Social welfare (million RMB)	Taicang	3931.55	3927.30	0.11
	Zhenjiang	10391.15	10118.18	2.70
	Nanjing	5383.00	5472.64	-1.64
	Wuhu	3436.66	3381.98	1.62
	Wuhan	4808.29	4805.03	0.07
	Chongqing	9722.07	9716.26	0.06
	Yibin	452.24	454.56	-0.51
	Total	38124.95	37875.95	0.66

Note: Relative change = (coordinated – independent)/ independent × 100%.

5.2.2. Port capacity investments under different port operating regimes

The congestion delays of Taicang port and Zhenjiang port are currently more serious than other ports. In order to alleviate the port congestion delays, the municipal governments of

these two cities are recently planning to expand their port capacities. Fig. 7a and b shows the changes of the total social welfare of the corridor system and the individual social welfares of Taicang and Zhenjiang ports for various combinations of their capacity expansions under the coordinated and independent regimes, respectively.

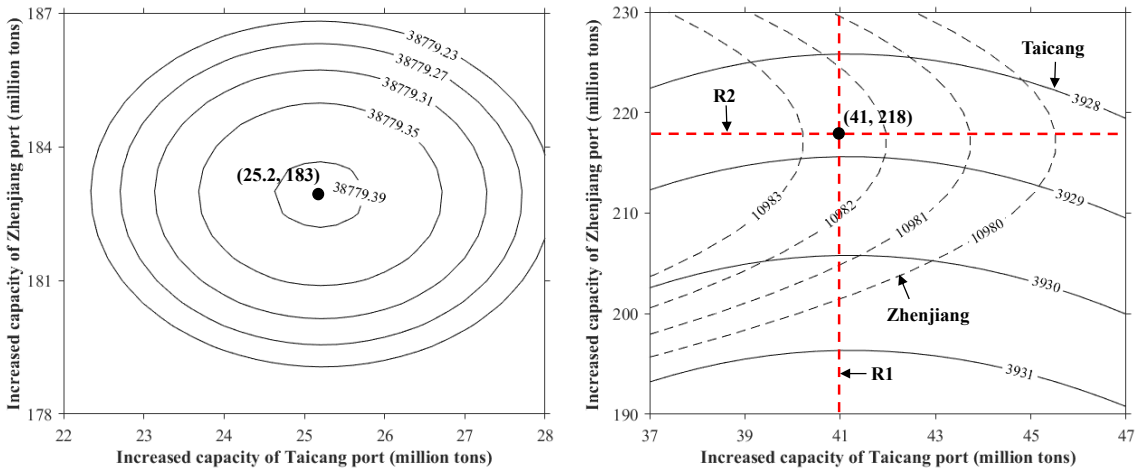

(a) (b)

Fig. 7. Changes of total social welfare of the system and individual social welfares (million RMB) of Taicang and Zhenjiang ports with port capacity expansions under different regimes: (a) coordinated regime, and (b) independent regime.

It can be observed in Fig. 7a that for the coordinated regime, the optimal capacity expansion of Taicang port is 25.2 million tons and the optimal capacity expansion of Zhenjiang port is 183 million tons, leading to the maximum total system social welfare of 38779.397 million RMB. For the independent regime, as the capacity of one port increases, the social welfare of its rival port decreases. The curve R1 (R2) is the response of optimal capacity investment of Taicang (Zhenjiang) port to the capacity change of the competitive Zhenjiang (Taicang) port. When the capacity investments of Taicang and Zhenjiang ports are, respectively, 41 million tons and 218 million tons, which are the intersection of two response curves, the game between these two ports reaches Nash equilibrium and no port is willing to change its decision on capacity investment. It can be noted that the optimal capacity expansions of Taicang and Zhenjiang ports under the independent regime are 15.8 and 35 million tons larger than those under the coordinated regime, respectively. This is because the local government under the independent regime would like to provide high-quality services through expanding bigger port capacities to compete for hinterland cargo market with its rivals. As a result of port competition, there may exist a risk of resource waste due to excessive port capacity

investment for the independent regime. Consequently, in practice the decisions on the port capacity expansion and port operating regime should be carefully made.

5.2.3. Waterway depth investments under different port operating regimes

In order to look at the effects of investing in the waterway depth under the coordinated and independent regimes, we conduct numerical experiments by changing the waterway depth H_i of port i from 0 to 1.0 m. Fig. 8a plots the change in the total social welfare of the system under the coordinated regime. Fig. 8b plots the change in the individual social welfare of each port under the independent regime.

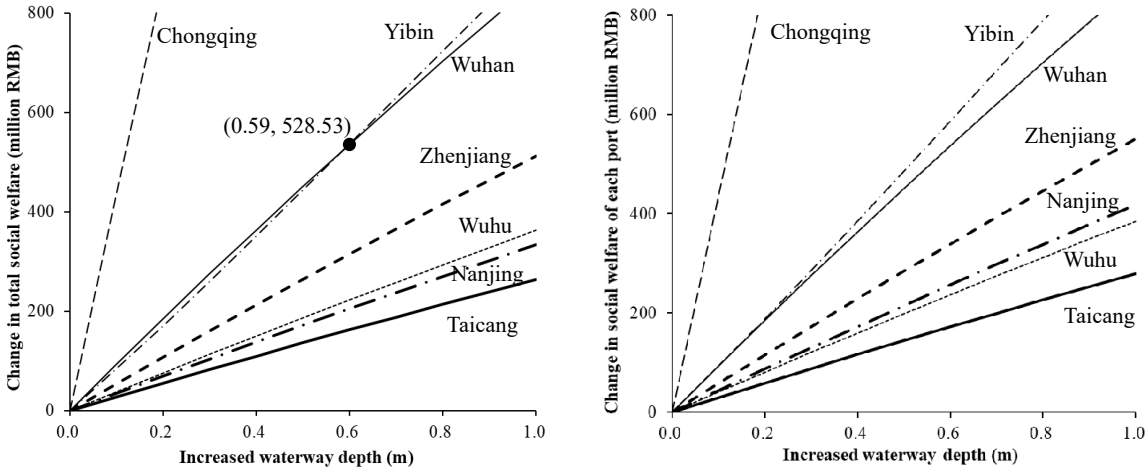

(a) (b)

Fig. 8. Changes of total social welfare of the system and individual social welfare of each port under different regimes: (a) coordinated regime, and (b) independent regime.

It can be seen in Fig. 8a and b that investing in the waterway depth of Chongqing port (Taicang port) can lead to the largest (smallest) change in the total social welfare and its individual social welfare regardless of the coordinated or independent regime. This means that the marginal investment values (or shadow values) of Chongqing port and Taicang port are the highest and the lowest in terms of the change of (total/individual) social welfare per unit waterway depth investment, respectively. Thereby, Chongqing port can be considered as the first choice for investment in the waterway depth, while Taicang port as the last choice, regardless of the port operating regime adopted.

It can also be seen that for the independent regime, the shadow values of Yibin and Wuhan ports are the second and third largest among all ports, implying that Yibin and Wuhan ports can be considered as the second and third investment choices, respectively. However, for the coordinated regime, Wuhan port is a better choice for investment than Yibin port if the additional invested waterway depth is less than 0.59 m, and Yibin port is a better choice, otherwise. In addition, the priority rankings of investment for Nanjing and Wuhu ports are just reverse for the coordinated and independent regimes. Specifically, Nanjing and Wuhu ports under the coordinated regime have the reverse second and third investment priorities, respectively. However, their investment priorities under the independent regime become the reverse third and second ones, respectively.

According to the above discussions, we can obtain a general rule about the order of waterway depth investment of inland river ports along the Yangtze River: the upstream major ports (e.g., Chongqing, Yibin, Wuhan) can be chosen for waterway depth investment first, and then the downstream major ports (e.g., Zhenjiang, Nanjing, Wuhu, Taicang), regardless of the operating regimes adopted. More importantly, the framework can be used to conduct other policy or investment decisions, e.g., to simulate the market outcomes when a new port is invested, when capacities at selected ports are to be expanded, or when transport costs to selected ports are reduced or increased (such as in the cases when a new road is built or additional toll charges are imposed). It can also be easily extended to the case when multiple ports are managed by a group (e.g. port alliance), or selected ports are privatized (thus that their objectives are to maximize profits instead of local welfare).

6. Conclusion and further studies

This paper proposes a vertical-structure model for the strategic planning of ports in an inland river corridor. In the proposed model, the interactions among shippers, carriers, and port operators are explicitly considered, together with the effects of waterway depth, port congestion, and port competition on the hinterland cargo market. The port service charge, port capacity, waterway freight rate and ship fleet for each port in the inland river system are optimized. Two different port operating regimes are investigated and compared, i.e., the coordinated regime that maximizes total social welfare of the entire inland river corridor system, and the independent regime that maximizes the local social welfare of each individual

inland river port.

This study contributes to the literature and practical industry decision making in several ways. First, in terms of methodology it develops a more comprehensive model than previous studies, which can be used for the analysis of complex issues and scenarios, such as the effects of the waterway depth investment on the inland river port corridor system under coordinated vs. independent regimes. The model can analyze the cases of multiple ports, and reveal changes to individual ports (e.g. hinterland areas of upstream/downstream inland ports and thus in service coverage of river corridor). Second, in term of general findings for inland river port management, we have shown that the optimal capacity expansion of each port under the independent regime is always larger than that under the coordinated regime. This is because each independent government needs more port capacities to compete for hinterland cargo market with rivals. This conclusion may have very important implications for inland port investment and choice of regulation schemes. Regulation always comes with costs (e.g. regulation costs associated with tax collection, administration). When the cargo demand along the inland river is expected to grow substantially in coming years, limited over-investments may not be a major problem in the long term. In such a case, encouraging competition is a preferred solution than central management/coordination. However, if market growth is expected to be limited in the years to come, regulation cost is a less important issue compared to the wastes caused by excessive investments. In such a case, centralized regulation/coordination may be a preferred choice. Because such results are obtained under general modelling assumptions, they should hold for inland river shipping in general. Third, some specific conclusions have been obtained for the case of Yangtze River. For example, it is found that the priority order of waterway depth investment is to first invest in the upstream major ports and then the downstream major ports, regardless of the operating regimes adopted. This can be a useful investment guideline especially when a decision-maker can coordinate the strategy of investments along the inland river. In summary, the proposed models in this paper provide a useful tool for modeling the interactions among port operators, carriers, and shippers and for evaluating and designing various demand-side and/or supply-side policies.

Although the models proposed in this paper provide some useful insights for practical investment decisions and policy evaluation of inland river ports, some assumptions made should be relaxed in further studies.

(1) The cargo demand was assumed to be continuously distributed along the inland river. Such

an assumption may, to some extent, overly simplify the market reality. Moreover, the road in this paper was assumed to be uncongested. A discrete cargo demand distribution along the inland river corridor and road congestion may be considered in a further study.

(2) Only one ship type and one carrier were considered for each port. In reality, there may exist multiple ship types and multiple carriers at a port. It is, therefore, meaningful to extend the proposed models to take multiple ship types and multiple carriers into account.

(3) With continuing upgrading of the inland waterway, some inland river ports can accommodate larger ships and some sea ships can directly enter the inland river. It is meaningful to develop an integrated model for investigating the ship layout/scheduling issues of the combined river-sea transport (Konings, 2006), particularly considering the effects of upgrading of the inland river waterway.

(4) The proposed models were deterministic, and various random factors, such as uncertainties in cargo demand or/and port capacity, were not considered. In a further study, the effects of random factors should be incorporated through developing stochastic or robust models.

(5) This paper considered the inland river ports operated by central or local governments, aiming to maximize total or local social welfare. However, some inland river ports in Europe and North America are operated by private sectors, with an objective of maximizing their own profit. Therefore, there is a need to extend the models proposed in this paper to consider the profit maximization case in a future study.

References

Álvarez-SanJaime, Ó., Cantos-Sánchez, P., Moner-Colonques, R., Sempere-Monerris, J.J., 2015. The impact on port competition of the integration of port and inroad transport services. Transportation Research Part B 80, 291-302.

Amsden, A.H., Singh, A., 1994. The optimal degree of competition and dynamic efficiency in Japan and Korea. European Economic Review 38 (3-4), 941-951.

Basso, L.J., Zhang, A., 2007. Congestible facility rivalry in vertical structures. Journal of Urban Economics 61 (2), 218-237.

Blaug, M., 2001. Is competition such a good thing? Static efficiency versus dynamic efficiency. Review of Industrial Organization 19 (1), 37-48.

Brown, I.N., Aldridge, M.F., 2019. Power models and average ship parameter effects on marine emissions inventories. Journal of the Air & Waste Management Association 69

(6), 752-763.

Dai, Q., Yang, J.Q., Li, D., 2018. Modeling a three-mode hybrid port-hinterland freight intermodal distribution network with environmental consideration: The case of the Yangtze River Economic Belt in China. Sustainability 10 (9), 3081-3107.

Fan, A.L., Yin, X.Z., Yan, X.P., Sun, X., 2015. Study of energy efficient navigation method for inland ship: A cruise ship case. Presented at the 3rd International Conference on Transportation Information Safety, 437-441.

Hawdon, D., 1978. Tanker freight rates in the short and long run. Applied Economics 10, 203-217.

Homsombat, W., Yip, T.L., Yang, H.J., Fu, X.W., 2013. Regional cooperation and management of port pollution. Maritime Policy & Management 40 (5), 451-466.

Jiang, Y.L., Lu, J., Cai, Y.T., Zeng, Q.C., 2018. Analysis of the impacts of different modes of governance on inland waterway transport development on the Pearl River: The Yangtze River mode vs. the Pearl River mode. Journal of Transport Geography 71, 235-252.

Kaselimi, E.N., Notteboom, T.E., Borger, B.D., 2011. A game theoretical approach to competition between multi-user terminals: The impact of dedicated terminals. Maritime Policy and Management 38 (4), 395-414.

Konings, R., 2006. Hub-and-spoke networks in container-on-barge transport. Transportation Research Record 1963 (1), 23-32.

Li, Z.C., Lam, W.H.K., Wong, S.C., Sumalee, A., 2012. Design of a rail transit line for profit maximization in a linear transportation corridor. Transportation Research Part E 48 (1), 50-70.

Meng, Q., Wang, T., Wang, S., 2012. Short-term liner ship fleet planning with container transshipment and uncertain container shipment demand. European Journal of Operational Research 223 (1), 96-105.

Meng, Q., Wang, X., 2011. Intermodal hub-and-spoke network design: Incorporating multiple stakeholders and multi-type containers. Transportation Research Part B 45 (4), 724-742.

Merika, A., Merikas, A., Tsionas, M., Andrikopoulos, A., 2019. Exploring vessel-price dynamics: The case of the dry bulk market. Maritime Policy and Management 46 (3-4), 309-329.

Radmilovi, Z., Zobenica, R., Mara, V., 2011. River-sea shipping - competitiveness of various transport technologies. Journal of Transport Geography 19 (6), 1509-1516.

Sauri, S., 2006. Cost structure in a short sea shipping line. Journal of Maritime Research 3 (2), 53-66.

Sheng, D., Li, Z.C., Fu, X., 2017. Modeling the effects of unilateral and uniform emission regulations under carrier and port competition. Transportation Research Part E 101, 99-114.

Strang, G., 2006. Linear Algebra and Its Applications. Thomson, Brooks/Cole, Belmont, CA, USA.

Talley, W.K., Port Economics. London: Routledge, 2009.

Tan, Z., Li, W., Zhang, X., Yang, H., 2015. Service charge and capacity choice of an inland river port with location-dependent shipping cost and service congestion. Transportation Research Part E 76, 13-33.

Tan, Z., Meng, Q., Wang, F., Kuang, H.B., 2018. Strategic integration of the inland port and shipping service for the ocean carrier. Transportation Research Part E 110, 90-109.

Trujillo, L., Campos, J., Pérez, I., 2018. Competition vs. cooperation between neighbouring ports: a case study in Chile. Research in Transportation Business & Management 26, 100-108.

Wan, Y., Basso, L.J., Zhang, A., 2016. Strategic investments in accessibility under port competition and inter-regional coordination. Transportation Research Part B 93, 102-125.

Wan, Y., Jiang, C., Zhang, A., 2015. Airport congestion pricing and terminal investment: Effects of terminal congestion, passenger types, and concessions. Transportation Research Part B 82 (4), 91-113.

Wang, H., Meng, Q., Zhang, X., 2014b. Game-theoretical models for competition analysis in a new emerging liner container shipping market. Transportation Research Part B 70, 201-227.

Wang, H., Wang, S., Meng, Q., 2014a. Simultaneous optimization of schedule coordination and cargo allocation for liner container shipping networks. Transportation Research Part E 70, 261-273.

Wang, K., Yang, H., Hang, A., 2020. Seaport adaptation to climate change-related disasters: terminal operator market structure and inter-and intra-port co-opetition. Spatial Economic Analysis 15 (3), 311-335.

Wang, K., Zhang, A., 2018. Climate change, natural disasters and adaptation investments: Inter-and intra-port competition and cooperation. Transportation Research Part B 117, 158-189.

Wang, X.C., Meng, Q., 2019. Optimal price decisions for joint ventures between port operators and shipping lines under the congestion effect. European Journal of

Operational Research 273 (2), 695-707.

Witte, P., Wiegmans, B., Oort, F.V., Spit, T., 2012. Chokepoints in corridors: Perspectives on bottlenecks in the European transport network. Research in Transportation Business & Management 5, 57-66.

Witte, P., Wiegmans, B., Oort, F.V., Spit, T., 2014. Governing inland ports: A multi-dimensional approach to addressing inland port-city challenges in European transport corridors. Journal of Transport Geography 36, 42-52.

Xiao, Y., Ng, A.K., Yang, H., Fu, X., 2012. An analysis of the dynamics of ownership, capacity investments and pricing structure of ports. Transport Reviews 32 (5), 629-652.

Xing, H., Han, Z.T., Duan, S.L., Huang, L.Z., 2016. Analysis on characteristics of ship power parameters for world merchant fleet. Journal of Dalian Maritime University 42 (3), 37-43.

Xing, W., Liu, Q., Chen, G.J., 2018. Pricing strategies for port competition and cooperation. Maritime Policy & Management 45 (2), 260-277.

Zerny, A., Höffler, F., Mun, S.I., 2014. Hub port competition and welfare effects of strategic privatization. Economics of Transportation 3 (3), 211-220.

Zlatoper, T.J., Austrian, Z., 1989. Freight transportation demand: A survey of recent econometric studies. Transportation 16 (1), 27-46.

Appendix A: Definition of variables and parameters

Table A.1 Notation.

Symbol	Definition	Baseline value
D_i	Location of port i (km)	—
H_i	Waterway depth of port i (m)	—
K_i	Design capacity of port i (tons/year)	—
$q^0(x)$	Annual potential cargo demand density at location x (tons/km/year)	—
$q_i(x)$	Annual density of actual cargo demand originating at location x and transshipping at port i	—
q_1	Gradient of cargo demand density along inland river corridor (tons/km^2)	—
Q_i	Annual actual total cargo volume of port i (tons/year)	—
S_i	Indifference location between adjacent ports i and i+1 (km)	—
t_i	Voyage time per unit of distance for ships of port i (h/km)	—
τ_i	Service charge per unit of cargo of port i (RMB/ton)	—
p_i	Waterway freight rate of one ton of cargo per unit of distance of carrier i (RMB/ton-km)	—
V_i	Average ship size of carrier i (tons)	—
γ	Average load factor of ships (%)	90%
n_i	Number of ships of carrier i	—
ω_i	Number of times that the ship V_i visits port i per year (or frequency)	—
c^R	Freight rate of road transport (RMB/ton-km)	0.50
t_0^R	Road transport time per unit of distance (h/km)	0.01
α_1	Value of road transport time perceived by shippers (RMB/h/ton-km)	5.0
α_2	Value of port congestion delay perceived by shippers (RMB/h/ton-km)	3.5
α_3	Value of waterway transport time perceived by shippers (RMB/h/ton-km)	1.0
λ_0	A positive parameter	0.5
λ_1	Scale economy of voyage time per unit of cargo with regard to ship size	0.28
η	A positive parameter (ton/m)	1000
f_0	Fixed operating cost of one ton of cargo per unit of distance (RMB/ton-km)	0.005
f_1	Marginal operating cost of one ton of cargo per unit of distance (RMB/ton^2-km)	2.0×10^{-7}
f_2	Fixed component of acquisition cost per ship (RMB)	120000
f_3	Variable component of acquisition cost per ship (RMB/ton)	10
ξ	Demand elasticity parameter	—
b	Maximum acceptable full transport cost for shippers (RMB/ton)	470
μ_0	Fixed cost of port dredging investment (Million RMB)	6.0
μ_1	Variable cost of port dredging investment (Million RMB/ m)	1.0
β_0	Fixed cost of port capacity investment (Million RMB)	3.0
β_1	Variable cost of port capacity investment (RMB/ton)	5.0

Appendix B: Proof of Lemma 1

We check the Hessian matrix $H_N(\pi_i^{(c)})$ of objective function $\pi_i^{(c)}$ in Eq. (14) with respect to the waterway freight rate vector **p**.

$$\begin{cases} \dfrac{\partial^2 \pi_i^{(c)}}{\partial p_i^2} = \dfrac{-q_0 (D_i)^2 exp\left(-\xi(p_i + \alpha_3 \lambda_0 V_i^{-\lambda_1}) D_i\right)}{4(c_v^R + \alpha_1 t_0^R)} \begin{pmatrix} 16 - 4\exp\left(-\xi(c^R + \alpha_1 t_0^R)(D_i - S_{i-1})\right) - 4\exp\left(-\xi(c^R + \alpha_1 t_0^R)(S_i - D_i)\right) \\ -\xi(p_i D_i - \tau_i - \delta_i) \begin{pmatrix} 8 - \exp\left(-\xi(c^R + \alpha_1 t_0^R)(D_i - S_{i-1})\right) \\ -\exp\left(-\xi(c^R + \alpha_1 t_0^R)(S_i - D_i)\right) \end{pmatrix} \end{pmatrix} < 0, \\ \dfrac{\partial^2 \pi_i^{(c)}}{\partial p_{i-1}^2} = -(p_i D_i - \tau_i - \delta_i) \dfrac{q_0 \xi (D_{i-1})^2 \exp\left(-\xi\left((c^R + \alpha_1 t_0^R)(D_i - S_{i-1}) + (p_i + \alpha_3 \lambda_0 V_i^{-\lambda_1}) D_i\right)\right)}{4(c^R + \alpha_1 t_0^R)} < 0, \\ \dfrac{\partial^2 \pi_i^{(c)}}{\partial p_{i+1}^2} = -(p_i D_i - \tau_i - \delta_i) \dfrac{q_0 \xi (D_{i+1})^2 \exp\left(-\xi\left((c^R + \alpha_1 t_0^R)(S_i - D_i) + (p_i + \alpha_3 \lambda_0 V_i^{-\lambda_1}) D_i\right)\right)}{4(c^R + \alpha_1 t_0^R)} < 0, \\ \dfrac{\partial^2 \pi_i^{(c)}}{\partial p_j^2} = 0, \quad j \neq i-1, i, i+1, \end{cases} \tag{B.1}$$

$$\begin{cases} \dfrac{\partial^2 \pi_i^{(c)}}{\partial p_i \partial p_{i-1}} = \dfrac{q_0 D_{i-1} D_i \left(2 - \xi(p_i D_i - \tau_i - \delta_i)\right) \exp\left(-\xi\left((c^R + \alpha_1 t_0^R)(D_i - S_{i-1}) + (p_i + \alpha_3 \lambda_0 V_i^{-\lambda_1}) D_i\right)\right)}{4(c^R + \alpha_1 t_0^R)} > 0, \\ \dfrac{\partial^2 \pi_i^{(c)}}{\partial p_i \partial p_{i+1}} = \dfrac{q_0 D_i D_{i+1} \left(2 - \xi(p_i D_i - \tau_i - \delta_i)\right) \exp\left(-\xi\left((c^R + \alpha_1 t_0^R)(S_i - D_i) + (p_i + \alpha_3 \lambda_0 V_i^{-\lambda_1}) D_i\right)\right)}{4(c^R + \alpha_1 t_0^R)} > 0, \\ \dfrac{\partial^2 \pi_i^{(c)}}{\partial p_i \partial p_j} = 0, \quad j \neq i-1, i, i+1, \\ \dfrac{\partial^2 \pi_i^{(c)}}{\partial p_j \partial p_k} = 0, \quad j, k \neq i, \end{cases} \tag{B.2}$$

where $\delta_i = (f_0 - f_1 V_i) D_i + \dfrac{1}{\gamma \omega_i} \left(\dfrac{f_2}{V_i} + f_3 \right)$.

The Hessian matrix $H_N(\pi_i^{(c)})$ with regard to the waterway freight rate vector **p** thus is

$$H_N(\pi_i^{(c)}) = \begin{bmatrix} 0 & \cdots & 0 & 0 & 0 & \cdots & 0 \\ \vdots & \ddots & \vdots & \vdots & \vdots & \iddots & \vdots \\ 0 & \cdots & \dfrac{\partial^2 \pi_i^{(c)}}{\partial p_{i-1}^2} & \dfrac{\partial^2 \pi_i^{(c)}}{\partial p_{i-1} \partial p_i} & 0 & \cdots & 0 \\ 0 & \cdots & \dfrac{\partial^2 \pi_i^{(c)}}{\partial p_i \partial p_{i-1}} & \dfrac{\partial^2 \pi_i^{(c)}}{\partial p_i^2} & \dfrac{\partial^2 \pi_i^{(c)}}{\partial p_i \partial p_{i+1}} & \cdots & 0 \\ 0 & \cdots & 0 & \dfrac{\partial^2 \pi_i^{(c)}}{\partial p_{i+1} \partial p_i} & \dfrac{\partial^2 \pi_i^{(c)}}{\partial p_{i+1}^2} & \cdots & 0 \\ \vdots & \iddots & \vdots & \vdots & \vdots & \ddots & \vdots \\ 0 & \cdots & 0 & 0 & 0 & \cdots & 0 \end{bmatrix}. \tag{B.3}$$

In order to show the negative definiteness of $H_N(\pi_i^{(c)})$, one only needs to check the negative definiteness of the associated quadratic form $Y^T H_N(\pi_i^{(c)}) Y$, where the superscript "T" denotes the transpose of a vector and Y is a column vector with $Y = (y_1, y_2, \cdots, y_N)^T$. The quadratic form $Y^T H_N(\pi_i^{(c)}) Y$ can be expressed as

$$
\begin{aligned}
Y^T H_N(\pi_i^{(c)})Y = &-q_0\left(\frac{2-\xi(p_iD_i-\tau_i-\delta_i)}{4(c^R+\alpha_1 t_0^R)}\right)\left(\chi_1(D_{i-1}y_{i-1}-D_iy_i)^2+\chi_1(D_iy_i-D_{i+1}y_{i+1})^2\right)\\
&-q_0\left(\frac{\xi(p_iD_i-\tau_i-\delta_i)-1}{4(c^R+\alpha_1 t_0^R)}\right)\left(\chi_2(D_{i-1}y_{i-1})^2+\chi_1(D_{i+1}y_{i+1})^2\right)\\
&-\frac{q_0\exp\left(-\xi(p_i+\alpha_3\lambda_0V_i^{-\lambda_1})D_i\right)}{2(c_v^R+\alpha_1 t_0^R)}\left(8-3\chi_3-\xi(p_iD_i-\tau_i-\delta_i)(4-\chi_3)\right)(D_iy_i)^2,
\end{aligned}
\tag{B.4}
$$

where

$$
\begin{cases}
\chi_1=\exp\left(-\xi\left((c^R+\alpha_1 t_0^R)(S_i-D_i)+(p_i+\alpha_3\lambda_0V_i^{-\lambda_1})D_i\right)\right),\\
\chi_2=\exp\left(-\xi\left((c^R+\alpha_1 t_0^R)(D_i-S_{i-1})+(p_i+\alpha_3\lambda_0V_i^{-\lambda_1})D_i\right)\right),\\
\chi_3=\exp\left(-\xi(c^R+\alpha_1 t_0^R)(D_i-S_{i-1})\right)+\exp\left(-\xi(c^R+\alpha_1 t_0^R)(S_i-D_i)\right).
\end{cases}
\tag{B.5}
$$

From Eq. (16), one can derive $0<\xi(p_iD_i-\tau_i-\delta_i)<1$. Consequently, for any non-zero vector *Y*, the following inequality always holds

$$
Y^T H_N(\pi_i^{(c)})Y<0. \tag{B.6}
$$

This means that the Hessian matrix $H_N(\pi_i^{(c)})$ is negative definite (Strang, 2006; Li et al., 2012), and thus $\pi_i^{(c)}$ is concave with respect to $p_1, p_2, \cdots, p_N$.

The first-order partial derivatives of objective function $\pi_i^{(c)}$ with respect to ship size V_i is

$$
\begin{cases}
\dfrac{\partial\pi_i^{(c)}}{\partial V_i}=\dfrac{1}{\gamma\omega_i}\left(f_1D_i+\dfrac{f_2}{(V_i)^2}\right)Q_i+\dfrac{q_0\alpha_3\lambda_0\lambda_1V_i^{-\lambda_1-1}D_i(p_iD_i-\tau_i-\delta_i)\exp\left(-\xi(p_i+\alpha_3\lambda_0V_i^{-\lambda_1})D_i\right)}{2(c^R+\alpha_1 t_0^R)}\begin{pmatrix}4-\exp\left(-\xi(c^R+\alpha_1 t_0^R)(D_i-S_{i-1})\right)\\-\exp\left(-\xi(c^R+\alpha_1 t_0^R)(S_i-D_i)\right)\end{pmatrix}>0, i=1,2,\cdots,N-1\\
\dfrac{\partial\pi_N^{(c)}}{\partial V_N}=\dfrac{1}{\gamma\omega_i}\left(f_1D_N+\dfrac{f_2}{(V_N)^2}\right)Q_N+\dfrac{q_0\alpha_3\lambda_0\lambda_1V_N^{-\lambda_1-1}D_N(p_ND_N-\tau_N-\delta_N)\exp\left(-\xi(p_N+\alpha_3\lambda_0V_N^{-\lambda_1})D_N\right)}{2(c^R+\alpha_1 t_0^R)}\left(4-\exp\left(-\xi(c^R+\alpha_1 t_0^R)(D_N-S_{N-1})\right)\right)>0.
\end{cases}
\tag{B.7}
$$

For $V_i\geq 0$, $\dfrac{\partial\pi_i^{(c)}}{\partial V_i}$ is always larger than zero. Thus, as the ship size V_i increases, the objective function $\pi_i^{(c)}$ increases. This completes the proof.

Appendix C: Proof of Proposition 1

To analyze the effects of waterway freight rate p_i and road freight rate c^R on S_j and L_j, we set the partial derivatives of Eqs. (21) and (23) respectively with respect to p_i and c^R equal to zero and solving them simultaneously for $N = 3$. With the uniform cargo demand distribution $q_i(x) = q_0$, one can derive the expressions of $\partial S_j / \partial p_i$, $\partial L_j / \partial p_i$, $\partial S_j / \partial c^R$, and $\partial L_j / \partial c^R$ as follows:

$$\begin{cases} \dfrac{\partial S_0}{\partial p_1} = \rho(c^R + \alpha_1 t_0^R) D_1 \left(5(\alpha_2 q_0)^2 + 2\alpha_2 q_0 (c^R + \alpha_1 t_0^R)(3K_2 + 2K_3) + 4K_2 K_3 (c^R + \alpha_1 t_0^R)^2\right) K_1 > 0, \\ \dfrac{\partial S_1}{\partial p_1} = -2\rho(c^R + \alpha_1 t_0^R) D_1 \left((\alpha_2 q_0)^2 + \alpha_2 q_0 (c^R + \alpha_1 t_0^R)(3K_2 + K_3) + 2K_2 K_3 (c^R + \alpha_1 t_0^R)^2\right) K_1 < 0, \\ \dfrac{\partial S_2}{\partial p_1} = -2\rho(c^R + \alpha_1 t_0^R) D_1 \alpha_2 q_0 \left(\alpha_2 q_0 + (c^R + \alpha_1 t_0^R) K_3\right) K_1 < 0, \\ \dfrac{\partial S_3}{\partial p_1} = -2\rho(c^R + \alpha_1 t_0^R) D_1 (\alpha_2 q_0)^2 K_1 < 0. \end{cases} \tag{C.1}$$

$$\begin{cases} \dfrac{\partial S_0}{\partial p_2} = \rho(c^R + \alpha_1 t_0^R) D_2 \alpha_2 q_0 \left(3\alpha_2 q_0 + 2K_3 (c^R + \alpha_1 t_0^R)\right) K_2 > 0, \\ \dfrac{\partial S_1}{\partial p_2} = \rho(c^R + \alpha_1 t_0^R) D_2 \left(3(\alpha_2 q_0)^2 + 2\alpha_2 q_0 (c^R + \alpha_1 t_0^R)(3K_1 + K_3) + 4K_1 K_3 (c^R + \alpha_1 t_0^R)^2\right) K_2 > 0, \\ \dfrac{\partial S_2}{\partial p_2} = -4\rho(c^R + \alpha_1 t_0^R) D_2 \left((\alpha_2 q_0)^2 + \alpha_2 q_0 (c^R + \alpha_1 t_0^R)(K_1 + K_3) + K_1 K_3 (c^R + \alpha_1 t_0^R)^2\right) K_2 < 0, \\ \dfrac{\partial S_3}{\partial p_2} = -4\rho(c^R + \alpha_1 t_0^R) D_2 \alpha_2 q_0 \left(\alpha_2 q_0 + (c^R + \alpha_1 t_0^R) K_1\right) K_2 < 0. \end{cases} \tag{C.2}$$

$$\begin{cases} \dfrac{\partial S_0}{\partial p_3} = \rho(c^R + \alpha_1 t_0^R) D_3 (\alpha_2 q_0)^2 K_3 > 0, \\ \dfrac{\partial S_1}{\partial p_3} = \rho(c^R + \alpha_1 t_0^R) D_3 \alpha_2 q_0 \left(\alpha_2 q_0 + 2K_1 (c^R + \alpha_1 t_0^R)\right) K_3 > 0, \\ \dfrac{\partial S_2}{\partial p_3} = \rho(c^R + \alpha_1 t_0^R) D_3 \left((\alpha_2 q_0)^2 + 4\alpha_2 q_0 (c^R + \alpha_1 t_0^R)(K_1 + 2K_2) + 4K_1 K_2 (c^R + \alpha_1 t_0^R)^2\right) K_3 > 0, \\ \dfrac{\partial S_3}{\partial p_3} = -2\rho(c^R + \alpha_1 t_0^R) D_3 \left(3(\alpha_2 q_0)^2 + 4\alpha_2 q_0 (c^R + \alpha_1 t_0^R)(K_1 + K_2) + 4K_1 K_2 (c^R + \alpha_1 t_0^R)^2\right) K_3 < 0. \end{cases} \tag{C.3}$$

$$\begin{cases} \dfrac{\partial L_1}{\partial p_1} = -\rho(c^R + \alpha_1 t_0^R) D_1 \left(7(\alpha_2 q_0)^2 + 6\alpha_2 q_0 (c^R + \alpha_1 t_0^R)(2K_2 + K_3) + 8K_2 K_3 (c^R + \alpha_1 t_0^R)^2\right) < 0 \\ \dfrac{\partial L_2}{\partial p_1} = 2\rho(c^R + \alpha_1 t_0^R)^2 D_1 \left(3\alpha_2 q_0 + 2K_3 (c^R + \alpha_1 t_0^R)\right) K_1 K_2 > 0, \\ \dfrac{\partial L_3}{\partial p_1} = 2\rho(c^R + \alpha_1 t_0^R)^2 D_1 \alpha_2 q_0 K_1 K_3 > 0. \end{cases} \tag{C.4}$$

$$\begin{cases} \dfrac{\partial L_1}{\partial p_2} = 2\rho(c^R + \alpha_1 t_0^R)^2 D_2 \left(3\alpha_2 q_0 + 2K_3(c^R + \alpha_1 t_0^R)\right) K_1 K_2 > 0, \\ \dfrac{\partial L_2}{\partial p_2} = -\rho(c^R + \alpha_1 t_0^R) D_2 \left(7(\alpha_2 q_0)^2 + 2\alpha_2 q_0 (c^R + \alpha_1 t_0^R)(5K_1 + 3K_3) + 8K_1 K_3 (c^R + \alpha_1 t_0^R)^2\right) K_2 < 0, \\ \dfrac{\partial L_3}{\partial p_2} = 4\rho(c^R + \alpha_1 t_0^R)^2 D_2 (\alpha_2 q_0 + K_1) K_2 K_3 > 0. \end{cases} \tag{C.5}$$

$$\begin{cases} \dfrac{\partial L_1}{\partial p_3} = 2\rho(c^R + \alpha_1 t_0^R)^2 D_3 \alpha_2 q_0 K_1 K_3 > 0, \\ \dfrac{\partial L_2}{\partial p_3} = 4\rho(c^R + \alpha_1 t_0^R)^2 D_3 \left(\alpha_2 q_0 + K_1(c^R + \alpha_1 t_0^R)\right) K_2 K_3 > 0, \\ \dfrac{\partial L_3}{\partial p_3} = -\rho(c^R + \alpha_1 t_0^R) D_3 \left(7(\alpha_2 q_0)^2 + 4\alpha_2 q_0 (c^R + \alpha_1 t_0^R)(3K_1 + 4K_2) + 12K_1 K_2 (c^R + \alpha_1 t_0^R)^2\right) K_3 < 0. \end{cases} \tag{C.6}$$

To analyze the effects of road freight rate c^R on S_j and L_j, we set the partial derivatives of Eqs. (9) and (10) with respect to c^R, yielding

$$\begin{cases} \dfrac{\partial S_0}{\partial c^R} = -\dfrac{1}{2(c^R)^2}\left(\dfrac{\alpha_2 Q_1}{K_1} + (p_1 + \alpha_3 \lambda_0 V_1^{-\lambda_1}) D_1\right) < 0, \\ \dfrac{\partial S_i}{\partial c^R} = -\dfrac{1}{2(c^R)^2}\left(\dfrac{\alpha_2 Q_{i+1}}{K_{i+1}} - \dfrac{\alpha_2 Q_i}{K_i} + (p_{i+1} + \alpha_3 \lambda_0 V_{i+1}^{-\lambda_1}) D_{i+1} - (p_i + \alpha_3 \lambda_0 V_i^{-\lambda_1}) D_i\right), \ i = 1, 2, \\ \dfrac{\partial S_3}{\partial c^R} = -\dfrac{b - (p_3 + \alpha_3 \lambda_0 V_3^{-\lambda_1}) D_3 - \dfrac{\alpha_2 Q_3}{K_3}}{(c^R)^2} < 0. \end{cases} \tag{C.7}$$

$$\begin{cases} \dfrac{\partial L_i}{\partial c^R} = -\dfrac{1}{2(c^R)^2}\left(\begin{array}{l} \dfrac{\alpha_2 Q_{i+1}}{K_{i+1}} - \dfrac{2\alpha_2 Q_i}{K_i} + \dfrac{\alpha_2 Q_{i-1}}{K_{i-1}} + (p_{i+1} + \alpha_3 \lambda_0 V_{i+1}^{-\lambda_1}) D_{i+1} \\ -2(p_i + \alpha_3 \lambda_0 V_i^{-\lambda_1}) D_i + (p_{i-1} + \alpha_3 \lambda_0 V_{i-1}^{-\lambda_1}) D_{i-1} \end{array}\right), \ i = 1, 2, \\ \dfrac{\partial L_3}{\partial c^R} = -\dfrac{1}{2(c^R)^2}\left(2b - \dfrac{3\alpha_2 Q_3}{K_3} + \dfrac{\alpha_2 Q_2}{K_2} - 3(p_3 + \alpha_3 \lambda_0 V_3^{-\lambda_1}) D_3 + (p_2 + \alpha_3 \lambda_0 V_2^{-\lambda_1}) D_2\right). \end{cases} \tag{C.8}$$

It should be pointed out that the signs of $\partial S_i / \partial c^R, i = 1, 2$ and $\partial L_i / \partial c^R, i = 1, 2, 3$ are ambiguous. The above results are summarized in Table 2. This completes the proof.

Appendix D: Proof of Proposition 2

The first-order partial derivatives of $\pi_i^{(c)}$ with respect to p_i is

$$\begin{cases} \dfrac{\partial \pi_i^{(c)}}{\partial p_i} = D_i Q_i - (p_i D_i - \tau_i - \delta_i)\dfrac{q_0 D_i}{c^R + \alpha_1 t_0^R}, i = 1, 2, \cdots, N-1, \\ \dfrac{\partial \pi_N^{(c)}}{\partial p_N} = D_N Q_N - (p_N D_N - \tau_N - \delta_N)\dfrac{3q_0 D_N}{2(c^R + \alpha_1 t_0^R)}. \end{cases} \tag{D.1}$$

Letting $\dfrac{\partial \pi_i^{(c)}}{\partial p_i}$ be equal to zero for the case of $N = 2$, one can then obtain

$$\begin{cases} p_1 = \dfrac{(c^R + \alpha_1 t_0^R)(-D_1 + 7D_2) + 12(\tau_1 + \delta_1) + 3(\tau_2 + \delta_2) + \alpha_3(-11 t_1 D_1 + 3 t_2 D_2) + 2b}{23 D_1}, \\ p_2 = \dfrac{(c^R + \alpha_1 t_0^R)(-4D_1 + 5D_2) + 2(\tau_1 + \delta_1) + 12(\tau_2 + \delta_2) + \alpha_3(2 t_1 D_1 - 11 t_2 D_2) + 8b}{23 D_2}, \end{cases} \tag{D.2}$$

The Jacobian matrix of p_i with regard to τ_i is thus

$$J = \begin{bmatrix} \dfrac{\partial p_1}{\partial \tau_1} & \dfrac{\partial p_1}{\partial \tau_2} \\ \dfrac{\partial p_2}{\partial \tau_1} & \dfrac{\partial p_2}{\partial \tau_2} \end{bmatrix} = \begin{bmatrix} \dfrac{12}{23 D_1} & \dfrac{3}{23 D_1} \\ \dfrac{2}{23 D_2} & \dfrac{12}{23 D_2} \end{bmatrix}. \tag{D.3}$$

When $N = 3$, one can obtain

$$\begin{cases} p_1 = \dfrac{(c^R + \alpha_1 t_0^R)(-6D_1 + 22D_2 + 7D_3) + 46(\tau_1 + \delta_1) + 12(\tau_2 + \delta_2) + 3(\tau_3 + \delta_3) - \alpha_3(40 t_1 D_1 - 12 t_2 D_2 - 3 t_3 D_3) + 2b}{86 D_1}, \\ p_2 = \dfrac{(c^R + \alpha_1 t_0^R)(-12D_1 + D_2 + 14D_3) + 6(\tau_1 + \delta_1) + 24(\tau_2 + \delta_2) + 6(\tau_3 + \delta_3) + \alpha_3(6 t_1 D_1 - 19 t_2 D_2 + 6 t_3 D_3) + 4b}{43 D_2}, \\ p_3 = \dfrac{(c^R + \alpha_1 t_0^R)(-4D_1 - 14D_2 + 19D_3) + 2(\tau_1 + \delta_1) + 8(\tau_2 + \delta_2) + 45(\tau_3 + \delta_3) + \alpha_3(2 t_1 D_1 + 8 t_2 D_2 - 41 t_3 D_3) + 30b}{86 D_3}. \end{cases} \tag{D.4}$$

The Jacobian matrix of p_i with regard to τ_i is thus

$$J = \begin{bmatrix} \dfrac{\partial p_1}{\partial \tau_1} & \dfrac{\partial p_1}{\partial \tau_2} & \dfrac{\partial p_1}{\partial \tau_3} \\ \dfrac{\partial p_2}{\partial \tau_1} & \dfrac{\partial p_2}{\partial \tau_2} & \dfrac{\partial p_2}{\partial \tau_3} \\ \dfrac{\partial p_3}{\partial \tau_1} & \dfrac{\partial p_3}{\partial \tau_2} & \dfrac{\partial p_3}{\partial \tau_3} \end{bmatrix} = \begin{bmatrix} \dfrac{23}{43 D_1} & \dfrac{6}{43 D_1} & \dfrac{3}{86 D_1} \\ \dfrac{6}{43 D_2} & \dfrac{23}{43 D_2} & \dfrac{6}{43 D_2} \\ \dfrac{1}{43 D_3} & \dfrac{4}{43 D_3} & \dfrac{45}{86 D_3} \end{bmatrix}. \tag{D.5}$$

By comparing the rows and columns of the Jacobian matrices respectively, one can immediately obtain the results of Proposition 2.

Appendix E: Proof of Proposition 3

When $N = 2$, the Jacobian matrices of τ_i^{CO} and τ_i^{ID} with respect to waterway depth H_i are

$$J^{CO} = \begin{bmatrix} \frac{\partial \tau_1^{CO}}{\partial H_1} & \frac{\partial \tau_1^{CO}}{\partial H_2} \\ \frac{\partial \tau_2^{CO}}{\partial H_1} & \frac{\partial \tau_2^{CO}}{\partial H_2} \end{bmatrix} = \begin{bmatrix} 0 & \frac{1}{4}\left(\eta D_2\left(\alpha_3\lambda_0\lambda_1(\eta H_2)^{-\lambda_1-1}+f_1\right)+\frac{f_2}{\gamma\omega_2\eta(H_2)^2}\right) \\ \frac{17}{100}\left(\eta D_1\left(\alpha_3\lambda_0\lambda_1(\eta H_1)^{-\lambda_1-1}+f_1\right)+\frac{f_2}{\gamma\omega_1\eta(H_1)^2}\right) & 0 \end{bmatrix}. \quad \text{(E.1)}$$

$$J^{ID} = \begin{bmatrix} \frac{\partial \tau_1^{ID}}{\partial H_1} & \frac{\partial \tau_1^{ID}}{\partial H_2} \\ \frac{\partial \tau_2^{ID}}{\partial H_1} & \frac{\partial \tau_2^{ID}}{\partial H_2} \end{bmatrix} = \begin{bmatrix} \frac{21}{500}\left(\eta D_1\left(\alpha_3\lambda_0\lambda_1(\eta H_1)^{-\lambda_1-1}+f_1\right)+\frac{f_2}{\gamma\omega_1\eta(H_1)^2}\right) & \frac{-11}{1000}\left(\eta D_2\left(\alpha_3\lambda_0\lambda_1(\eta H_2)^{-\lambda_1-1}+f_1\right)+\frac{f_2}{\gamma\omega_2\eta(H_2)^2}\right) \\ \frac{-7}{1000}\left(\eta D_1\left(\alpha_3\lambda_0\lambda_1(\eta H_1)^{-\lambda_1-1}+f_1\right)+\frac{f_2}{\gamma\omega_1\eta(H_1)^2}\right) & \frac{21}{500}\left(\eta D_2\left(\alpha_3\lambda_0\lambda_1(\eta H_2)^{-\lambda_1-1}+f_1\right)+\frac{f_2}{\gamma\omega_2\eta(H_2)^2}\right) \end{bmatrix}. \quad \text{(E.2)}$$

When $N = 3$, the Jacobian matrices of τ_i^{CO} and τ_i^{ID} with respect to waterway depth H_i are

$$J^{CO} = \begin{bmatrix} \frac{\partial \tau_1^{CO}}{\partial H_1} & \frac{\partial \tau_1^{CO}}{\partial H_2} & \frac{\partial \tau_1^{CO}}{\partial H_3} \\ \frac{\partial \tau_2^{CO}}{\partial H_1} & \frac{\partial \tau_2^{CO}}{\partial H_2} & \frac{\partial \tau_2^{CO}}{\partial H_3} \\ \frac{\partial \tau_3^{CO}}{\partial H_1} & \frac{\partial \tau_3^{CO}}{\partial H_2} & \frac{\partial \tau_3^{CO}}{\partial H_3} \end{bmatrix}$$

$$= \begin{bmatrix} 0 & \frac{1}{4}\left(\eta D_2\left(\alpha_3\lambda_0\lambda_1(\eta H_2)^{-\lambda_1-1}+f_1\right)+\frac{f_2}{\gamma\omega_2\eta(H_2)^2}\right) & 0 \\ \frac{1}{4}\left(\eta D_1\left(\alpha_3\lambda_0\lambda_1(\eta H_1)^{-\lambda_1-1}+f_1\right)+\frac{f_2}{\gamma\omega_1\eta(H_1)^2}\right) & 0 & \frac{1}{4}\left(\eta D_3\left(\alpha_3\lambda_0\lambda_1(\eta H_3)^{-\lambda_1-1}+f_1\right)+\frac{f_2}{\gamma\omega_3\eta(H_3)^2}\right) \\ 0 & \frac{17}{100}\left(\eta D_2\left(\alpha_3\lambda_0\lambda_1(\eta H_2)^{-\lambda_1-1}+f_1\right)+\frac{f_2}{\gamma\omega_2\eta(H_2)^2}\right) & 0 \end{bmatrix}. \quad \text{(E.3)}$$

$$J^{ID} = \begin{bmatrix} \frac{\partial \tau_1^{ID}}{\partial H_1} & \frac{\partial \tau_1^{ID}}{\partial H_2} & \frac{\partial \tau_1^{ID}}{\partial H_3} \\ \frac{\partial \tau_2^{ID}}{\partial H_1} & \frac{\partial \tau_2^{ID}}{\partial H_2} & \frac{\partial \tau_2^{ID}}{\partial H_3} \\ \frac{\partial \tau_3^{ID}}{\partial H_1} & \frac{\partial \tau_3^{ID}}{\partial H_2} & \frac{\partial \tau_3^{ID}}{\partial H_3} \end{bmatrix}$$

$$= \begin{bmatrix} \frac{13}{200}\left(\eta D_1\left(\alpha_3\lambda_0\lambda_1(\eta H_1)^{-\lambda_1-1}+f_1\right)+\frac{f_2}{\gamma\omega_1\eta(H_1)^2}\right) & \frac{-9}{500}\left(\eta D_2\left(\alpha_3\lambda_0\lambda_1(\eta H_2)^{-\lambda_1-1}+f_1\right)+\frac{f_2}{\gamma\omega_2\eta(H_2)^2}\right) & \frac{-1}{200}\left(\eta D_3\left(\alpha_3\lambda_0\lambda_1(\eta H_3)^{-\lambda_1-1}+f_1\right)+\frac{f_2}{\gamma\omega_3\eta(H_3)^2}\right) \\ \frac{-31}{1000}\left(\eta D_1\left(\alpha_3\lambda_0\lambda_1(\eta H_1)^{-\lambda_1-1}+f_1\right)+\frac{f_2}{\gamma\omega_1\eta(H_1)^2}\right) & \frac{1}{10}\left(\eta D_2\left(\alpha_3\lambda_0\lambda_1(\eta H_2)^{-\lambda_1-1}+f_1\right)+\frac{f_2}{\gamma\omega_2\eta(H_2)^2}\right) & \frac{-4}{125}\left(\eta D_3\left(\alpha_3\lambda_0\lambda_1(\eta H_3)^{-\lambda_1-1}+f_1\right)+\frac{f_2}{\gamma\omega_3\eta(H_3)^2}\right) \\ \frac{-1}{500}\left(\eta D_1\left(\alpha_3\lambda_0\lambda_1(\eta H_1)^{-\lambda_1-1}+f_1\right)+\frac{f_2}{\gamma\omega_1\eta(H_1)^2}\right) & \frac{-1}{125}\left(\eta D_2\left(\alpha_3\lambda_0\lambda_1(\eta H_2)^{-\lambda_1-1}+f_1\right)+\frac{f_2}{\gamma\omega_2\eta(H_2)^2}\right) & \frac{11}{250}\left(\eta D_3\left(\alpha_3\lambda_0\lambda_1(\eta H_3)^{-\lambda_1-1}+f_1\right)+\frac{f_2}{\gamma\omega_3\eta(H_3)^2}\right) \end{bmatrix}. \quad \text{(E.4)}$$

By comparing the rows and columns of the Jacobian matrices respectively, one can immediately obtain the results of Proposition 3.

Appendix F: Proof of Proposition 4

When N = 2, the Jacobian matrices of p_i^{CO} and p_i^{ID} with respect to waterway depth H_i are as follows.

$$J^{CO}=\begin{bmatrix}\frac{\partial p_1^{CO}}{\partial H_1} & \frac{\partial p_1^{CO}}{\partial H_2}\\ \frac{\partial p_2^{CO}}{\partial H_1} & \frac{\partial p_2^{CO}}{\partial H_2}\end{bmatrix}=\begin{bmatrix}\frac{-12}{25\gamma\omega_1\eta(H_1)^2D_1}\left(\begin{matrix}D_1f_1\gamma\omega_1(\eta H_1)^2+f_2\\ -\frac{11}{12}D_1\alpha_3\lambda_0\lambda_1\gamma\omega_1(\eta H_1)^{1-\lambda_1}\end{matrix}\right) & 0\\ \frac{-1}{2500\gamma\omega_1\eta(H_1)^2D_2}\left(\begin{matrix}D_2f_1\gamma\omega_1(\eta H_1)^2+f_2\\ +D_1\alpha_3\lambda_0\lambda_1\gamma\omega_1(\eta H_1)^{1-\lambda_1}\end{matrix}\right) & \frac{-12}{25\gamma\omega_2\eta(H_2)^2D_2}\left(\begin{matrix}D_2f_1\gamma\omega_2(\eta H_2)^2+f_2\\ -D_2\alpha_3\lambda_0\lambda_1\gamma\omega_2(\eta H_2)^{1-\lambda_1}\end{matrix}\right)\end{bmatrix}. \tag{F.1}$$

$$J^{ID}=\begin{bmatrix}\frac{\partial p_1^{ID}}{\partial H_1} & \frac{\partial p_1^{ID}}{\partial H_2}\\ \frac{\partial p_2^{ID}}{\partial H_1} & \frac{\partial p_2^{ID}}{\partial H_2}\end{bmatrix}=\begin{bmatrix}\frac{-12}{25\gamma\omega_1\eta(H_1)^2D_1}\left(\begin{matrix}D_1f_1\gamma\omega_1(\eta H_1)^2+f_2\\ -\frac{11}{12}D_1\alpha_3\lambda_0\lambda_1\gamma\omega_1(\eta H_1)^{1-\lambda_1}\end{matrix}\right) & \frac{-3}{25\gamma\omega_2\eta(H_2)^2D_1}\left(\begin{matrix}D_2f_1\gamma\omega_2(\eta H_2)^2+f_2\\ +D_2\alpha_3\lambda_0\lambda_1\gamma\omega_2(\eta H_2)^{1-\lambda_1}\end{matrix}\right)\\ \frac{-2}{25\gamma\omega_1\eta(H_1)^2D_2}\left(\begin{matrix}D_1f_1\gamma\omega_1(\eta H_1)^2+f_2\\ +D_1\alpha_3\lambda_0\lambda_1\gamma\omega_1(\eta H_1)^{1-\lambda_1}\end{matrix}\right) & \frac{-12}{25\gamma\omega_2\eta(H_2)^2D_2}\left(\begin{matrix}D_2f_1\gamma\omega_2(\eta H_2)^2+f_2\\ -\frac{11}{12}D_2\alpha_3\lambda_0\lambda_1\gamma\omega_2(\eta H_2)^{1-\lambda_1}\end{matrix}\right)\end{bmatrix}. \tag{F.2}$$

When N = 3, the Jacobian matrices of p_i^{CO} and p_i^{ID} with respect to waterway depth H_i are as follows.

$$J^{CO}=\begin{bmatrix}\frac{\partial p_1^{CO}}{\partial H_1} & \frac{\partial p_1^{CO}}{\partial H_2} & \frac{\partial p_1^{CO}}{\partial H_3}\\ \frac{\partial p_2^{CO}}{\partial H_1} & \frac{\partial p_2^{CO}}{\partial H_2} & \frac{\partial p_2^{CO}}{\partial H_3}\\ \frac{\partial p_3^{CO}}{\partial H_1} & \frac{\partial p_3^{CO}}{\partial H_2} & \frac{\partial p_3^{CO}}{\partial H_3}\end{bmatrix}$$

$$=\begin{bmatrix}\frac{-43}{100\gamma\omega_1\eta(H_1)^2D_1}\left(\begin{matrix}D_1f_1\gamma\omega_1(\eta H_1)^2+f_2\\ -\eta D_1\alpha_3\lambda_0\lambda_1\gamma\omega_1(\eta H_1)^{1-\lambda_1}\end{matrix}\right) & \frac{-3}{10000\gamma\omega_2\eta(H_2)^2D_1}\left(\begin{matrix}D_2f_1\gamma\omega_2(\eta H_2)^2+f_2\\ +D_2\alpha_3\lambda_0\lambda_1\gamma\omega_2(\eta H_2)^{1-\lambda_1}\end{matrix}\right) & 0\\ 0 & \frac{-22}{50\gamma\omega_2\eta(H_2)^2D_2}\left(\begin{matrix}D_2f_1\gamma\omega_2(\eta H_2)^2+f_2\\ -\frac{21}{22}D_2\alpha_3\lambda_0\lambda_1\gamma\omega_2(\eta H_2)^{1-\lambda_1}\end{matrix}\right) & 0\\ 0 & \frac{-1}{2500\gamma\omega_2\eta(H_2)^2D_3}\left(\begin{matrix}D_2f_1\gamma\omega_2(\eta H_2)^2+f_2\\ +D_2\alpha_3\lambda_0\lambda_1\gamma\omega_2(\eta H_2)^{1-\lambda_1}\end{matrix}\right) & \frac{-43}{100\gamma\omega_3\eta(H_3)^2D_3}\left(\begin{matrix}D_3f_1\gamma\omega_3(\eta H_3)^2+f_2\\ -D_3\alpha_3\lambda_0\lambda_1\gamma\omega_3(\eta H_3)^{1-\lambda_1}\end{matrix}\right)\end{bmatrix}. \tag{F.3}$$

$$J^{ID}=\begin{bmatrix}\frac{\partial p_1^{ID}}{\partial H_1} & \frac{\partial p_1^{ID}}{\partial H_2} & \frac{\partial p_1^{ID}}{\partial H_3}\\ \frac{\partial p_2^{ID}}{\partial H_1} & \frac{\partial p_2^{ID}}{\partial H_2} & \frac{\partial p_2^{ID}}{\partial H_3}\\ \frac{\partial p_3^{ID}}{\partial H_1} & \frac{\partial p_3^{ID}}{\partial H_2} & \frac{\partial p_3^{ID}}{\partial H_3}\end{bmatrix}$$

$$=\begin{bmatrix}\frac{-43}{100\gamma\omega_1\eta(H_1)^2D_1}\left(\begin{matrix}D_1f_1\gamma\omega_1(\eta H_1)^2+f_2\\ -D_1\alpha_3\lambda_0\lambda_1\gamma\omega_1(\eta H_1)^{1-\lambda_1}\end{matrix}\right) & \frac{-3}{25\gamma\omega_2\eta(H_2)^2D_1}\left(\begin{matrix}D_2f_1\gamma\omega_2(\eta H_2)^2+f_2\\ +D_2\alpha_3\lambda_0\lambda_1\gamma\omega_2(\eta H_2)^{1-\lambda_1}\end{matrix}\right) & \frac{-1}{25\gamma\omega_3\eta(H_3)^2D_1}\left(\begin{matrix}D_3f_1\gamma\omega_3(\eta H_3)^2+f_2\\ +D_3\alpha_3\lambda_0\lambda_1\gamma\omega_3(\eta H_3)^{1-\lambda_1}\end{matrix}\right)\\ \frac{-3}{25\gamma\omega_1\eta(H_1)^2D_2}\left(\begin{matrix}D_1f_1\gamma\omega_1(\eta H_1)^2+f_2\\ +D_1\alpha_3\lambda_0\lambda_1\gamma\omega_1(\eta H_1)^{1-\lambda_1}\end{matrix}\right) & \frac{-22}{50\gamma\omega_2\eta(H_2)^2D_2}\left(\begin{matrix}D_2f_1\gamma\omega_2(\eta H_2)^2+f_2\\ -\frac{21}{22}D_2\alpha_3\lambda_0\lambda_1\gamma\omega_2(\eta H_2)^{1-\lambda_1}\end{matrix}\right) & \frac{-7}{50\gamma\omega_3\eta(H_3)^2D_2}\left(\begin{matrix}D_3f_1\gamma\omega_3(\eta H_3)^2+f_2\\ +D_3\alpha_3\lambda_0\lambda_1\gamma\omega_3(\eta H_3)^{1-\lambda_1}\end{matrix}\right)\\ \frac{-1}{50\gamma\omega_1\eta(H_1)^2D_3}\left(\begin{matrix}D_1f_1\gamma\omega_1(\eta H_1)^2+f_2\\ +D_1\alpha_3\lambda_0\lambda_1\gamma\omega_1(\eta H_1)^{1-\lambda_1}\end{matrix}\right) & \frac{-2}{25\gamma\omega_2\eta(H_2)^2D_3}\left(\begin{matrix}D_2f_1\gamma\omega_2(\eta H_2)^2+f_2\\ +D_2\alpha_3\lambda_0\lambda_1\gamma\omega_2(\eta H_2)^{1-\lambda_1}\end{matrix}\right) & \frac{-43}{100\gamma\omega_3\eta(H_3)^2D_3}\left(\begin{matrix}D_3f_1\gamma\omega_3(\eta H_3)^2+f_2\\ -D_3\alpha_3\lambda_0\lambda_1\gamma\omega_3(\eta H_3)^{1-\lambda_1}\end{matrix}\right)\end{bmatrix}. \tag{F.4}$$

By comparing the rows and columns of the Jacobian matrices respectively, one can immediately obtain the results of items (i) and (ii) in Proposition 4, together with $\partial p_i/\partial H_j<0$ if and only if $\dfrac{D_if_1\gamma\omega_i(\eta H_i)^2+f_i}{D_i\alpha_3\lambda_0\lambda_1\gamma\omega_i(\eta H_i)^{1-\lambda_1}}>1$.

Appendix G: Proof of Proposition 5

The first-order partial derivatives of SW_i^{CO} and SW_i^{ID} with respect to waterway depth H_i are as follows.

(1) For coordinated regime

When $N = 2$,

$$\begin{cases} \dfrac{\partial SW_1^{CO}}{\partial H_1} = \dfrac{q_0}{50(c^R+\alpha_1 t_0^R)}\left(\dfrac{\left(\eta D_1\left(11\alpha_3\lambda_0\lambda_1(\eta H_1)^{-\lambda_1-1}+13f_1\right)+\dfrac{13f_2}{\gamma\omega_1\eta(H_1)^2}\right)Q_1^{CO}}{25}+(p_1^{CO}D_1-\delta_1)\left(\eta D_1\left(25\alpha_3\lambda_0\lambda_1(\eta H_1)^{-\lambda_1-1}+24f_1\right)+\dfrac{24f_2}{\gamma\omega_1\eta(H_1)^2}\right)\right)-\mu_1>0, \\ \dfrac{\partial SW_1^{CO}}{\partial H_2} = -\dfrac{q_0}{50(c^R+\alpha_1 t_0^R)}\left((p_1^{CO}D_1-\delta_1)\left(\eta D_2\left(13\alpha_3\lambda_0\lambda_1(\eta H_2)^{-\lambda_1-1}+12f_1\right)+\dfrac{12f_2}{\gamma\omega_2\eta(H_2)^2}\right)\right)<0. \end{cases} \tag{G.1}$$

$$\begin{cases} \dfrac{\partial SW_2^{CO}}{\partial H_1} = -\dfrac{q_0}{50(c^R+\alpha_1 t_0^R)}\left(\dfrac{\left(\eta D_1\left(\alpha_3\lambda_0\lambda_1(\eta H_1)^{-\lambda_1-1}+f_1\right)+\dfrac{f_2}{\gamma\omega_1\eta(H_1)^2}\right)Q_2^{CO}}{2500}+2(p_2^{CO}D_2-\delta_2)\left(\eta D_1\left(7\alpha_3\lambda_0\lambda_1(\eta H_1)^{-\lambda_1-1}+6f_1\right)+\dfrac{6f_2}{\gamma\omega_1\eta(H_1)^2}\right)\right)<0, \\ \dfrac{\partial SW_2^{CO}}{\partial H_2} = \dfrac{q_0}{50(c^R+\alpha_1 t_0^R)}\left(\dfrac{\left(\eta D_2\left(12\alpha_3\lambda_0\lambda_1(\eta H_2)^{-\lambda_1-1}+13f_1\right)+\dfrac{13f_2}{\gamma\omega_2\eta(H_2)^2}\right)Q_2^{CO}}{25}+3(p_2^{CO}D_2-\delta_2)\left(\eta D_2\left(13\alpha_3\lambda_0\lambda_1(\eta H_2)^{-\lambda_1-1}+12f_1\right)+\dfrac{12f_2}{\gamma\omega_2\eta(H_2)^2}\right)\right)-\mu_1>0. \end{cases} \tag{G.2}$$

When $N = 3$,

$$\begin{cases} \dfrac{\partial SW_1^{CO}}{\partial H_1} = \dfrac{q_0}{100(c^R+\alpha_1 t_0^R)}\left(\dfrac{\left(\eta D_1\left(43\alpha_3\lambda_0\lambda_1(\eta H_1)^{-\lambda_1-1}+57f_1\right)+\dfrac{57f_2}{\gamma\omega_1\eta(H_1)^2}\right)Q_1^{CO}}{100}+(p_1^{CO}D_1-\delta_1)\left(\eta D_1\left(57\alpha_3\lambda_0\lambda_1(\eta H_1)^{-\lambda_1-1}+43f_1\right)+\dfrac{43f_2}{\gamma\omega_1\eta(H_1)^2}\right)\right)-\mu_1>0, \\ \dfrac{\partial SW_1^{CO}}{\partial H_2} = -\dfrac{q_0}{100(c^R+\alpha_1 t_0^R)}\left(\dfrac{3\left(\eta D_2\left(\alpha_3\lambda_0\lambda_1(\eta H_2)^{-\lambda_1-1}+f_1\right)+\dfrac{f_2}{\gamma\omega_2\eta(H_2)^2}\right)Q_1^{CO}}{10000}+(p_1^{CO}D_1-\delta_1)\left(\eta D_2\left(29\alpha_3\lambda_0\lambda_1(\eta H_2)^{-\lambda_1-1}+22f_1\right)+\dfrac{22f_2}{\gamma\omega_2\eta(H_2)^2}\right)\right)<0, \\ \dfrac{\partial SW_1^{CO}}{\partial H_3} = 0. \end{cases} \tag{G.3}$$

$$\begin{cases} \dfrac{\partial SW_2^{CO}}{\partial H_1} = -\dfrac{q_0(p_2^{CO}D_2-\delta_2)\left(\eta D_1\left(57\alpha_3\lambda_0\lambda_1(\eta H_1)^{-\lambda_1-1}+43f_1\right)+\dfrac{43f_2}{\gamma\omega_1\eta(H_1)^2}\right)}{200(c^R+\alpha_1 t_0^R)}<0, \\ \dfrac{\partial SW_2^{CO}}{\partial H_2} = \dfrac{q_0}{200(c^R+\alpha_1 t_0^R)}\left(\dfrac{\left(\eta D_2\left(21\alpha_3\lambda_0\lambda_1(\eta H_2)^{-\lambda_1-1}+28f_1\right)+\dfrac{28f_2}{\gamma\omega_2\eta(H_2)^2}\right)Q_2^{CO}}{50}+(p_2^{CO}D_2-\delta_2)\left(\eta D_2\left(116\alpha_3\lambda_0\lambda_1(\eta H_2)^{-\lambda_1-1}+88f_1\right)+\dfrac{88f_2}{\gamma\omega_2\eta(H_2)^2}\right)\right)-\mu_1>0, \\ \dfrac{\partial SW_2^{CO}}{\partial H_3} = -\dfrac{q_0(p_2^{CO}D_2-\delta_2)\left(\eta D_3\left(57\alpha_3\lambda_0\lambda_1(\eta H_3)^{-\lambda_1-1}+43f_1\right)+\dfrac{43f_2}{\gamma\omega_3\eta(H_3)^2}\right)}{200(c^R+\alpha_1 t_0^R)}<0. \end{cases} \tag{G.4}$$

$$\begin{cases} \dfrac{\partial SW_3^{CO}}{\partial H_1} = 0, \\ \dfrac{\partial SW_3^{CO}}{\partial H_2} = \dfrac{-q_0}{200(c^R+\alpha_1 t_0^R)}\left(\dfrac{0.04\left(\eta D_2\left(\alpha_3\lambda_0\lambda_1(\eta H_2)^{-\lambda_1-1}+f_1\right)+\dfrac{f_2}{\gamma\omega_2\eta(H_2)^2}\right)Q_3^{CO}}{100}+2(p_3^{CO}D_3-\delta_3)\left(\eta D_2\left(29\alpha_3\lambda_0\lambda_1(\eta H_2)^{-\lambda_1-1}+22f_1\right)+\dfrac{22f_2}{\gamma\omega_2\eta(H_2)^2}\right)\right)<0, \\ \dfrac{\partial SW_3^{CO}}{\partial H_3} = \dfrac{q_0}{200(c^R+\alpha_1 t_0^R)}\left(\dfrac{\left(\eta D_3\left(43\alpha_3\lambda_0\lambda_1(\eta H_3)^{-\lambda_1-1}+57f_1\right)+\dfrac{57f_2}{\gamma\omega_3\eta(H_3)^2}\right)Q_3^{CO}}{100}+(p_3^{CO}D_3-\delta_3)\left(\eta D_3\left(171\alpha_3\lambda_0\lambda_1(\eta H_3)^{-\lambda_1-1}+129f_1\right)+\dfrac{129f_2}{\gamma\omega_3\eta(H_3)^2}\right)\right)-\mu_1>0. \end{cases} \tag{G.5}$$

(2) For independent regime

When $N = 2$,

$$\begin{cases} \dfrac{\partial SW_1^{ID}}{\partial H_1} = \dfrac{q_0}{50(c^R + \alpha_1 t_0^R)} \left(\dfrac{\left(\eta D_1 \left(11\alpha_3\lambda_0\lambda_1 (\eta H_1)^{-\lambda_1 - 1} + 13 f_1 \right) + \dfrac{13 f_2}{\gamma\omega_1\eta (H_1)^2} \right) Q_1^{ID}}{25} + 2(p_1^{ID} D_1 - \delta_1) \left(\eta D_1 \left(13\alpha_3\lambda_0\lambda_1 (\eta H_1)^{-\lambda_1 - 1} + 11 f_1 \right) + \dfrac{11 f_2}{\gamma\omega_1\eta (H_1)^2} \right) \right) - \mu_1 > 0, \\ \dfrac{\partial SW_1^{ID}}{\partial H_2} = -\dfrac{q_0}{50(c^R + \alpha_1 t_0^R)} \left(\dfrac{3\left(\eta D_2 \left(\alpha_3\lambda_0\lambda_1 (\eta H_2)^{-\lambda_1 - 1} + f_1 \right) + \dfrac{f_2}{\gamma\omega_2\eta (H_2)^2} \right) Q_1^{ID}}{25} + 2(p_1^{ID} D_1 - \delta_1) \left(\eta D_2 \left(4\alpha_3\lambda_0\lambda_1 (\eta H_2)^{-\lambda_1 - 1} + 3 f_1 \right) + \dfrac{3 f_2}{\gamma\omega_2\eta (H_2)^2} \right) \right) < 0. \end{cases} \tag{G.6}$$

$$\begin{cases} \dfrac{\partial SW_2^{ID}}{\partial H_1} = -\dfrac{q_0}{50(c^R + \alpha_1 t_0^R)} \left(\dfrac{2\left(\eta D_1 \left(\alpha_3\lambda_0\lambda_1 (\eta H_1)^{-\lambda_1 - 1} + f_1 \right) + \dfrac{f_2}{\gamma\omega_1\eta (H_1)^2} \right) Q_2^{ID}}{25} + 2(p_2^{ID} D_2 - \delta_2) \left(\eta D_1 \left(4\alpha_3\lambda_0\lambda_1 (\eta H_1)^{-\lambda_1 - 1} + 3 f_1 \right) + \dfrac{3 f_2}{\gamma\omega_1\eta (H_1)^2} \right) \right) < 0, \\ \dfrac{\partial SW_2^{ID}}{\partial H_2} = \dfrac{q_0}{50(c^R + \alpha_1 t_0^R)} \left(\dfrac{\left(\eta D_2 \left(11\alpha_3\lambda_0\lambda_1 (\eta H_2)^{-\lambda_1 - 1} + 13 f_1 \right) + \dfrac{13 f_2}{\gamma\omega_2\eta (H_2)^2} \right) Q_2^{ID}}{25} + 3(p_2^{ID} D_2 - \delta_2) \left(\eta D_2 \left(13\alpha_3\lambda_0\lambda_1 (\eta H_2)^{-\lambda_1 - 1} + 11 f_1 \right) + \dfrac{11 f_2}{\gamma\omega_2\eta (H_2)^2} \right) \right) - \mu_1 > 0. \end{cases} \tag{G.7}$$

When $N = 3$,

$$\begin{cases} \dfrac{\partial SW_1^{ID}}{\partial H_1} = \dfrac{q_0}{100(c^R + \alpha_1 t_0^R)} \left(\dfrac{\left(\eta D_1 \left(43\alpha_3\lambda_0\lambda_1 (\eta H_1)^{-\lambda_1 - 1} + 57 f_1 \right) + \dfrac{57 f_2}{\gamma\omega_1\eta (H_1)^2} \right) Q_1^{ID}}{100} + (p_1^{ID} D_1 - \delta_1) \left(\eta D_1 \left(51\alpha_3\lambda_0\lambda_1 (\eta H_1)^{-\lambda_1 - 1} + 37 f_1 \right) + \dfrac{37 f_2}{\gamma\omega_1\eta (H_1)^2} \right) \right) - \mu_1 > 0, \\ \dfrac{\partial SW_1^{ID}}{\partial H_2} = -\dfrac{q_0}{100(c^R + \alpha_1 t_0^R)} \left(\dfrac{12\left(\eta D_2 \left(\alpha_3\lambda_0\lambda_1 (\eta H_2)^{-\lambda_1 - 1} + f_1 \right) + \dfrac{f_2}{\gamma\omega_2\eta (H_2)^2} \right) Q_1^{ID}}{100} + (p_1^{ID} D_1 - \delta_1) \left(\eta D_2 \left(17\alpha_3\lambda_0\lambda_1 (\eta H_2)^{-\lambda_1 - 1} + 10 f_1 \right) + \dfrac{10 f_2}{\gamma\omega_2\eta (H_2)^2} \right) \right) < 0, \\ \dfrac{\partial SW_1^{ID}}{\partial H_3} = \dfrac{-q_0}{100(c^R + \alpha_1 t_0^R)} \left(\dfrac{4\left(\eta D_3 \left(\alpha_3\lambda_0\lambda_1 (\eta H_3)^{-\lambda_1 - 1} + f_1 \right) + \dfrac{f_2}{\gamma\omega_3\eta (H_3)^2} \right) Q_1^{ID}}{100} + 3(p_1^{ID} D_1 - \delta_1) \left(\eta D_3 \left(\alpha_3\lambda_0\lambda_1 (\eta H_3)^{-\lambda_1 - 1} + f_1 \right) + \dfrac{f_2}{\gamma\omega_3\eta (H_3)^2} \right) \right) < 0. \end{cases} \tag{G.8}$$

$$\begin{cases} \dfrac{\partial SW_2^{ID}}{\partial H_1} = -\dfrac{q_0}{200(c^R + \alpha_1 t_0^R)} \left(6\left(\eta D_1 \left(\alpha_3\lambda_0\lambda_1 (\eta H_1)^{-\lambda_1 - 1} + f_1 \right) + \dfrac{f_2}{\gamma\omega_1\eta (H_1)^2} \right) Q_2^{ID} + (p_2^{ID} D_2 - \delta_2) \left(\eta D_1 \left(35\alpha_3\lambda_0\lambda_1 (\eta H_1)^{-\lambda_1 - 1} + 21 f_1 \right) + \dfrac{21 f_2}{\gamma\omega_1\eta (H_1)^2} \right) \right) < 0, \\ \dfrac{\partial SW_2^{ID}}{\partial H_2} = \dfrac{q_0}{200(c^R + \alpha_1 t_0^R)} \left(\dfrac{\left(\eta D_2 \left(21\alpha_3\lambda_0\lambda_1 (\eta H_2)^{-\lambda_1 - 1} + 28 f_1 \right) + \dfrac{28 f_2}{\gamma\omega_2\eta (H_2)^2} \right) Q_2^{ID}}{50} + (p_2^{ID} D_2 - \delta_2) \left(\eta D_2 \left(96\alpha_3\lambda_0\lambda_1 (\eta H_2)^{-\lambda_1 - 1} + 68 f_1 \right) + \dfrac{68 f_2}{\gamma\omega_2\eta (H_2)^2} \right) \right) - \mu_1 > 0, \\ \dfrac{\partial SW_2^{ID}}{\partial H_3} = -\dfrac{q_0}{200(c^R + \alpha_1 t_0^R)} \left(\dfrac{7\left(\eta D_3 \left(\alpha_3\lambda_0\lambda_1 (\eta H_3)^{-\lambda_1 - 1} + f_1 \right) + \dfrac{f_2}{\gamma\omega_3\eta (H_3)^2} \right) Q_2^{ID}}{50} + (p_2^{ID} D_2 - \delta_2) \left(\eta D_3 \left(33\alpha_3\lambda_0\lambda_1 (\eta H_3)^{-\lambda_1 - 1} + 19 f_1 \right) + \dfrac{19 f_2}{\gamma\omega_3\eta (H_3)^2} \right) \right) < 0. \end{cases} \tag{G.9}$$

$$\begin{cases} \dfrac{\partial SW_3^{ID}}{\partial H_1} = -\dfrac{q_0}{200(c^R + \alpha_1 t_0^R)} \left(\dfrac{2\left(\eta D_1 \left(\alpha_3\lambda_0\lambda_1 (\eta H_1)^{-\lambda_1 - 1} + f_1 \right) + \dfrac{f_2}{\gamma\omega_1\eta (H_1)^2} \right) Q_3^{ID}}{100} + 6(p_3^{ID} D_3 - \delta_3) \left(\eta D_1 \left(\alpha_3\lambda_0\lambda_1 (\eta H_1)^{-\lambda_1 - 1} + f_1 \right) + \dfrac{f_2}{\gamma\omega_1\eta (H_1)^2} \right) \right) < 0, \\ \dfrac{\partial SW_3^{ID}}{\partial H_2} = -\dfrac{q_0}{200(c^R + \alpha_1 t_0^R)} \left(\dfrac{8\left(\eta D_2 \left(\alpha_3\lambda_0\lambda_1 (\eta H_2)^{-\lambda_1 - 1} + f_1 \right) + \dfrac{f_2}{\gamma\omega_2\eta (H_2)^2} \right) Q_3^{ID}}{100} + 2(p_3^{ID} D_3 - \delta_3) \left(\eta D_2 \left(17\alpha_3\lambda_0\lambda_1 (\eta H_2)^{-\lambda_1 - 1} + 10 f_1 \right) + \dfrac{10 f_2}{\gamma\omega_2\eta (H_2)^2} \right) \right) < 0, \\ \dfrac{\partial SW_3^{ID}}{\partial H_3} = \dfrac{q_0}{200(c^R + \alpha_1 t_0^R)} \left(\dfrac{\left(\eta D_3 \left(43\alpha_3\lambda_0\lambda_1 (\eta H_3)^{-\lambda_1 - 1} + 57 f_1 \right) + \dfrac{57 f_2}{\gamma\omega_3\eta (H_3)^2} \right) Q_3^{ID}}{100} + (p_3^{ID} D_3 - \delta_3) \left(\eta D_3 \left(157\alpha_3\lambda_0\lambda_1 (\eta H_3)^{-\lambda_1 - 1} + 115 f_1 \right) + \dfrac{f_2}{\gamma\omega_3\eta (H_3)^2} \right) \right) - \mu_1 > 0. \end{cases} \tag{G.10}$$